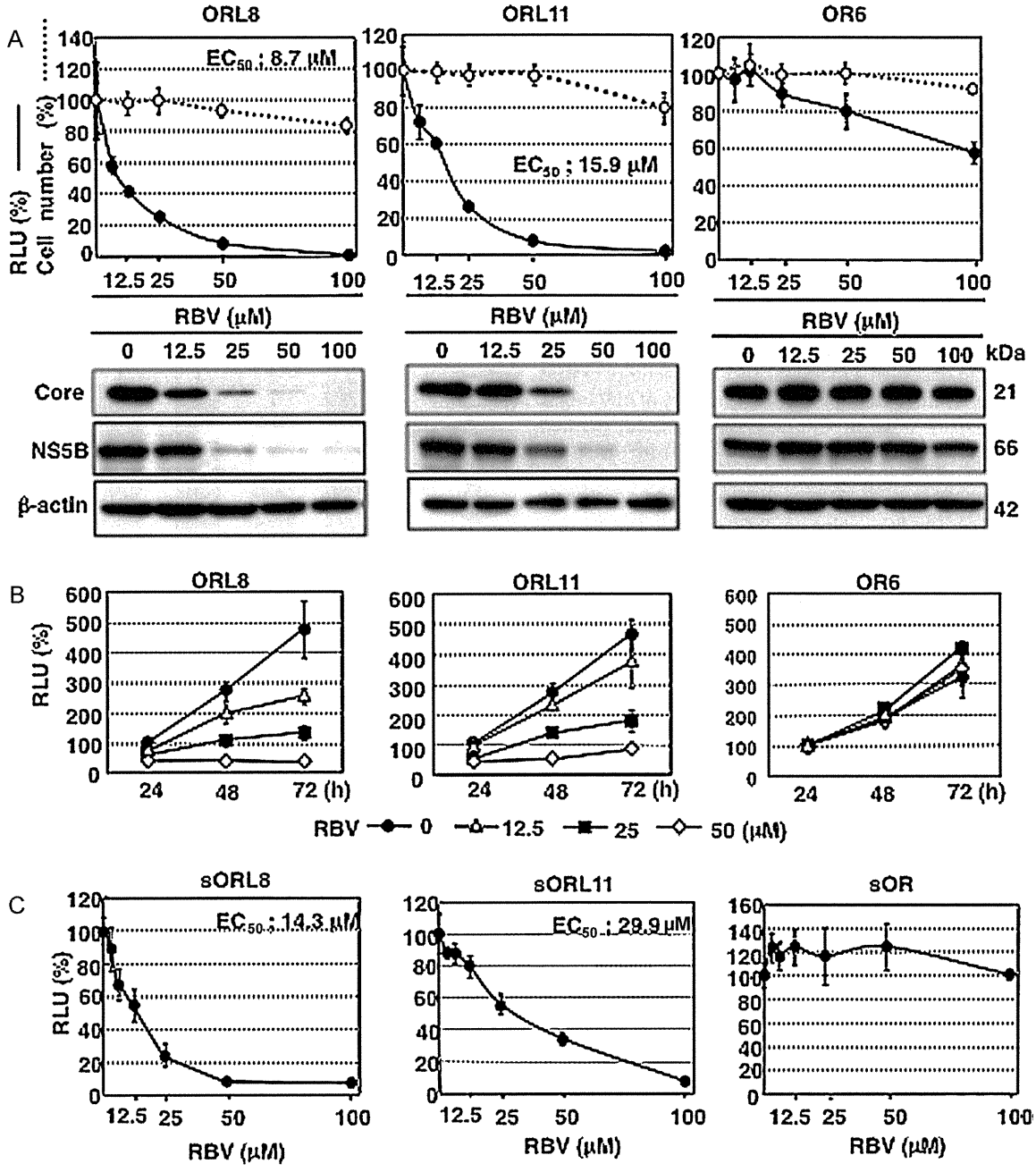

Fig. 1. Anti-HCV activity of RBV detected in the ORL8 and ORL11 system. (A) RBV sensitivities on genome-length HCV RNA replication in ORL8, ORL11, and OR6. The ORL8, ORL11 and OR6 cells were treated with RBV for 72 h, and then an RL assay (bold line in the upper panel) was performed. The relative luciferase activity (RLU) (%) calculated at each point, when the level of luciferase activity in non-treated cells was assigned to be 100% is presented here. The cell number (dotted line in the upper panel) at each concentration was determined as described in Section 2. Western blot analysis of RBV-treated ORL8, ORL11, and OR6 cells for HCV proteins, Core and NS5B, was also performed (lower panel). (B) Time-dependent anti-HCV activity of RBV. The ORL8, ORL11, and OR6 cells were treated with RBV, and an RL assay was performed at 24, 48, and 72 h after the treatment. The RLU (%) calculated at each time point, when the luciferase activity of non-treated cells at 24 h was assigned to be 100%, is shown. (C) Anti-HCV activity of RBV was observed in Li23-derived replicon assay systems (sORL8 and sORL11), but not in HuH-7-derived replicon assay system (sOR). RBV treatment and RL assay were performed as described for panel A.

two parts (6.0 kb covering 5′-UTR to NS3 and 6.1 kb covering NS3 to NS5B) and the two PCR products were subcloned for the sequence analysis as described above.

2.9. RNA interference and quantitative RT-PCR

SiRNA duplexes targeting the coding regions of human IMPDH1 (Dhamacon; catalog no. M-009687-01) and IMPDH2 (Dharmacon; catalog no. M-004330-02) were chemically synthesized. SiRNA duplex non-targeting (Dharmacon; catalog no. D-001206-13) was also used as a control. ORL8 cells were transfected with the indicated siRNA duplexes using Oligofectamine (Invitrogen) (Dansako et al., 2007). Extraction of total RNA and quantitative RT-PCR analysis for HCV RNA were performed by real-time LightCycler PCR as described previously (Ikeda et al., 2005).

2.10. Statistical analysis

Statistical comparison of the luciferase activities between the treatment groups and controls was performed using the Student's

t-test. *P* values of less than 0.05 were considered statistically significant.

3. Results

3.1. Anti-HCV activity of RBV was clearly observed in the Li23-derived assay systems, but not in the HuH-7-derived assay system

Recently we demonstrated that Li23-derived assay systems (ORL8 and ORL11), in which genome-length HCV RNA (O strain of genotype 1b) encoding RL robustly replicates, were frequently more sensitive to anti-HCV reagents such as IFNs and statins than the corresponding HuH-7-derived assay system (OR6) (Kato et al., 2009). Since we had observed a marginal anti-HCV activity of RBV in OR6 system, we assumed that the anti-HCV activity of RBV might also be illuminated by ORL8 or ORL11 system. Indeed, marked differences were observed between OR6 and both of the other assay systems: RBV at clinically achievable concentrations effectively inhibited HCV RNA replication in both ORL8 and ORL11, but not in OR6 (Fig. 1A). The EC_{50} values of RBV in ORL8, ORL11, and OR6 were 8.7, 15.9, and >100 μM, respectively, without suppression of cell growth (upper panels in Fig. 1A). These pronounced differences in the anti-HCV activity of RBV were confirmed by Western blot analysis (lower panels in Fig. 1A). In addition, time course assays revealed that the anti-HCV activity of RBV was dose- and time-dependent in ORL8 and ORL11, but not in OR6 (Fig. 1B). We next examined the activity of RBV using polyclonal cell-based assay systems (sORL8, sORL11, and sOR (Ikeda et al., 2005)) harboring HCV replicon RNA. The results revealed that the EC_{50} values of RBV in sORL8 and sORL11 were 14.3 and 29.9 μM, respectively, whereas RBV showed no anti-HCV activity in sOR (Fig. 1C), suggesting that the anti-HCV activity of RBV was not either a clone-specific or genome-length HCV RNA-specific phenomenon. Moreover, we demonstrated by Western blot (upper panel of Fig. 2) and quantitative RT-PCR (lower panel of Fig. 2) analyses that RBV suppressed HCV RNA replication in HCV-JFH1-infected ORL8c cells, but not in HCV-JFH1-infected RSc cells, which HCV could infect and efficiently replicate within (Ariumi et al., 2007; Kato et al., 2009). These results also indicate that only the Li23-derived assay system can illuminate the anti-HCV activity of RBV.

3.2. An ENT inhibitor cancelled anti-HCV activity of RBV

As one possible explanation for the pronounced differences in RBV activity between the Li23- and HuH-7-derived assay systems, we considered that the efficiencies in the cellular uptake of RBV might have differed between the two types of cells. To date, two families of nucleoside transporter proteins have been identified: the ENT family (ENT1, ENT2, and ENT3) and the concentrative nucleotide transporter (CNT) family (CNT1, CNT2, and CNT3) (Pastor-Anglada et al., 2005). Two recent reports showed that ENT1 and CNT3 might be responsible for RBV uptake in HuH-7 cells (Ibarra and Pfeiffer, 2009), and that ENT1, but not ENT2 or CNTs, is a major RBV uptake transporter in human hepatocytes (Fukuchi et al., 2010). To test these points, we first examined the effects of an ENT inhibitor, NBMPR, and a CNT inhibitor, phloridzin dihydrate, on the anti-HCV activity of RBV (50 μM; 90% effective concentration [EC_{90}]) in ORL8 system. The results revealed that 5 μM NBMPR partially attenuated the anti-HCV activity of RBV in ORL8 (Fig. 3A). The marginal activity of RBV was also not changed in OR6 system treated with these transporter inhibitors (data not shown). A significant dose-dependency of the cancellation by NBMPR was also observed in ORL8 (Fig. 3B). Since we observed a lack of expression of CNT family members in ORL8 cells (data not shown), these

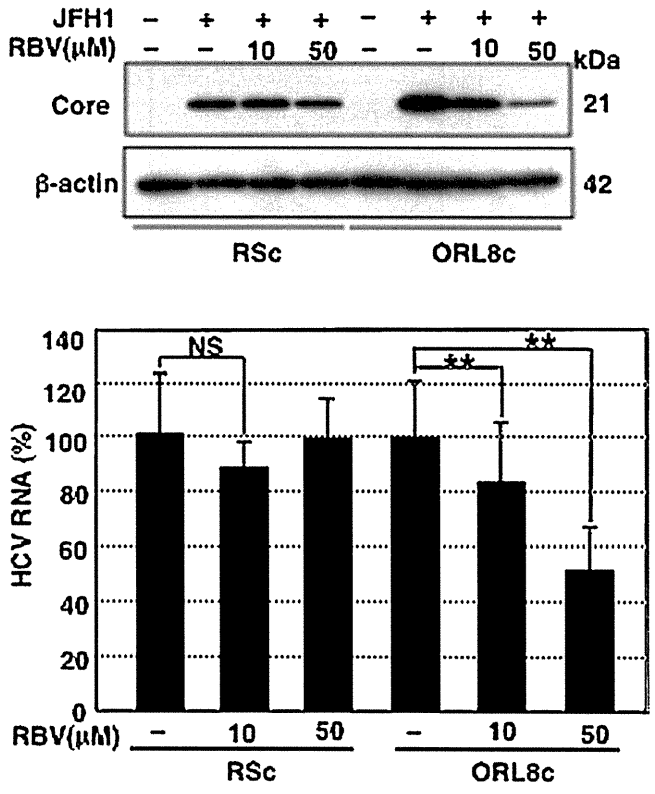

Fig. 2. RBV inhibited HCV production in JFH1-infected ORL8c cells, but not in JFH1-infected RSc cells. JFH1-infected ORL8c and RSc cells were treated with RBV for 72 h, and subjected to Western blot analysis using anti-Core or β-actin antibody (upper panel), and to quantitative RT-PCR analysis (lower panel). Asterisks indicate significant differences compared to the control treatment. $^{**}P<0.01$; NS, not significant.

results suggest that cellular uptake of RBV is mediated by ENT member(s). Accordingly, we next examined the levels of ENT mRNAs in ORL8 and OR6 cells. However, the expression levels of ENT1, ENT2, and ENT3 mRNAs were comparable between ORL8 and OR6 cells (Fig. 3C). In addition, sequence analysis of ENT1, ENT2, and ENT3 mRNAs (data not shown) and Western blot analysis of ENT1 protein (Fig. 3D) revealed no differences between the two cell lines. These results suggest that the expression levels of ENT members are not associated with the differences in RBV activity.

3.3. RBV did not act as a mutagen in HCV RNA replication

Since the suppressive effect of RBV on HCV RNA replication was clearly observed in ORL8 system, we expected that ORL8 cells would be suitable for analysis of the anti-HCV mechanism of RBV. In regard to the anti-HCV mechanism of RBV, several groups have proposed that RBV (50–400 μM) acts as an RNA mutagen and induces error catastrophe in HCV RNA replication (Contreras et al., 2002; Zhou et al., 2003). Therefore, we first examined whether or not error catastrophe theory is involved in the anti-HCV activity of RBV observed in ORL8 system. To test the mutagenic effect of RBV, ORL8 cells were treated with or without RBV (50 μM; EC_{90} level in ORL8 system) for 72 h, and then genome-length HCV RNA from the ORL8 cells was amplified by RT-PCR. We performed HCV quasispecies analysis by sequencing of RL to the Neo^R, NS5A, and NS5B regions using at least 10 independent clones for each region. To estimate the mutation rate, the total number of mutations and the ratio of nonsynonymous to synonymous mutations in each region were determined by comparison with the parental HCV sequences (Kato et al., 2009). The results revealed that the overall mutation rate and the ratio of nonsynonymous to synonymous mutations in each

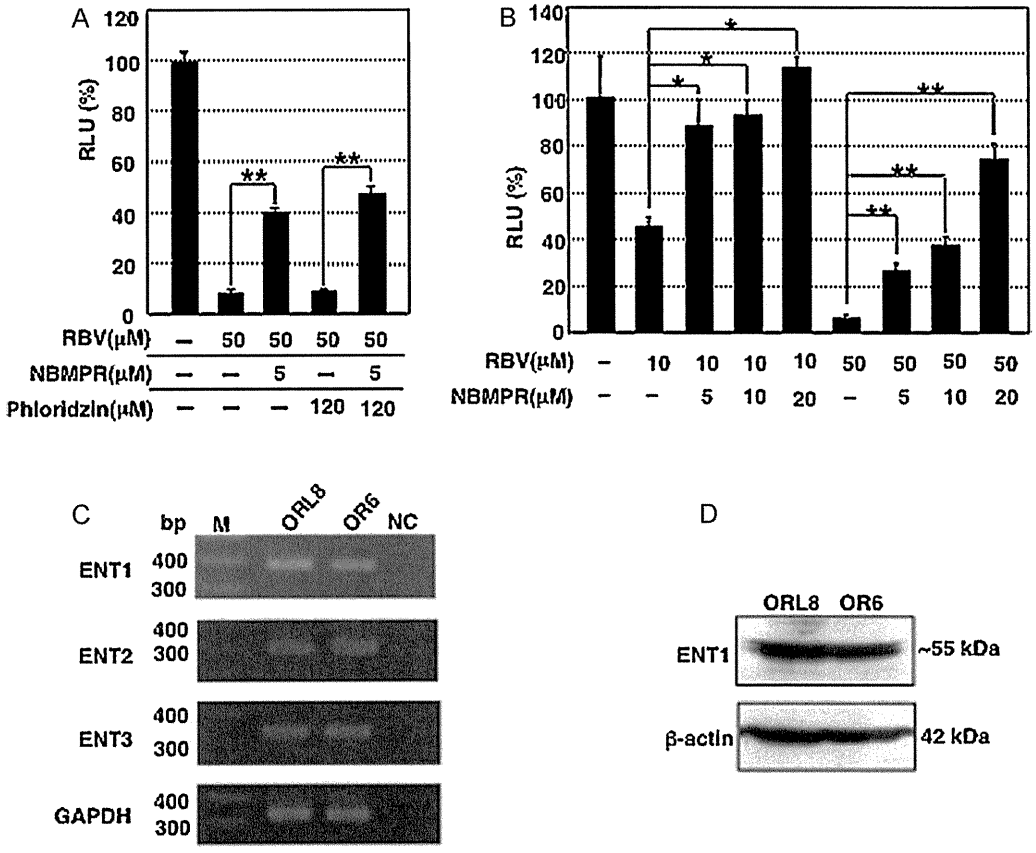

Fig. 3. An ENT inhibitor abolished anti-HCV activity of RBV. (A) An ENT inhibitor, NBMPR, canceled the anti-HCV activity of RBV in ORL8. ORL8 cells were pretreated with NBMPR and/or phloridzin dihydrate for 30 min, and then treated with RBV for 72 h, after which an RL assay was performed. Asterisks indicate significant differences compared to the control treatment. $^{**}P < 0.01$. (B) Dose-dependent cancellation by NBMPR of the activity of RBV. ORL8 cells were pretreated with NBMPR for 30 min, and then treated with RBV for 72 h, after which an RL assay was performed. Asterisks indicate significant differences compared to the control treatment. $^{*}P < 0.05$; $^{**}P < 0.01$. (C) RT-PCR analysis of ENTs. Total RNAs prepared from ORL8 and OR6 cells were subjected to RT-PCR using the primer sets for ENT1, ENT2, ENT3, and GAPDH as described in Section 2. RT-PCR products were detected by staining with ethidium bromide after 3% agarose gel electrophoresis. (D) Western blot analysis of ORL8 and OR6 cells for ENT1. The primary antibody used was ENT1. β-actin was used as a control for the amount of protein loaded per lane.

region were not increased irrespective of the presence or absence of RBV treatment (Table 1). To confirm that mutation frequencies given in Table 1 are overwhelmingly above the error level associated with the PCR, we sequenced independent five clones (6.0 kb covering 5′-UTR to NS3 and 6.1 kb covering NS3 to NS5B) obtained by PCR using KOD-plus DNA polymerase and a plasmid containing the parental HCV sequences (Kato et al., 2009) as a template. No mutations were detected in these sequenced clones, indicating that KOD-plus DNA polymerase possesses extremely high fidelity, and suggesting that the mutations obtained in the present study are not produced by the errors associated with the PCR. Therefore, these results indicate that RBV does not act as a mutagen in HCV RNA replication in ORL8 cells, and suggest that the anti-HCV activity of RBV (EC_{50}; 8.7 μM) observed in ORL8 system is not due to the induction of error catastrophe in the HCV RNA genome.

3.4. RBV did not activate the IFN-signaling pathway

Regarding HCV, Liu et al. (Liu et al., 2007) have reported that RBV (40–500 μM) enhances the IFN-signaling pathway in in vitro cell culture systems. Furthermore, a recent report showed that RBV improved early responses to PEG-IFN through enhanced IFN signaling in the treatment of patients with chronic hepatitis (Feld et al., 2010). In that study, it was shown that the RBV concentration in patients at day 3 was correlated with IP-10 induction at 12 h, but only in patients with an adequate first phase viral decline (Feld et al., 2010). Therefore, we expected that RBV would enhance the IFN-signaling pathway in our new cell culture system. Accordingly, we first examined the effect of RBV in combination with IFN-α on HCV RNA replication using ORL8 system. OR6 system was also used for purpose of comparison. The results showed that RBV had an additive effect in decreasing HCV RNA replica-

Table 1
Mutation frequencies in RL-Neo^R, NS5A, and NS5B regions.

Region	Condition	Total no. of clones	Total no. of mutations	Nonsynonymous/synonymous substitutions (ratio)
RL-Neo^R (1953 nts)	Control	12	59	39/20 (1.95)
	RBV (50 μM)	12	49	31/18 (1.72)
NS5A (1341 nts)	Control	10	35	24/11 (2.18)
	RBV (50 μM)	10	36	24/12 (2.00)
NS5B (1773 nts)	Control	10	10	3/7 (0.43)
	RBV (50 μM)	10	9	2/7 (0.29)

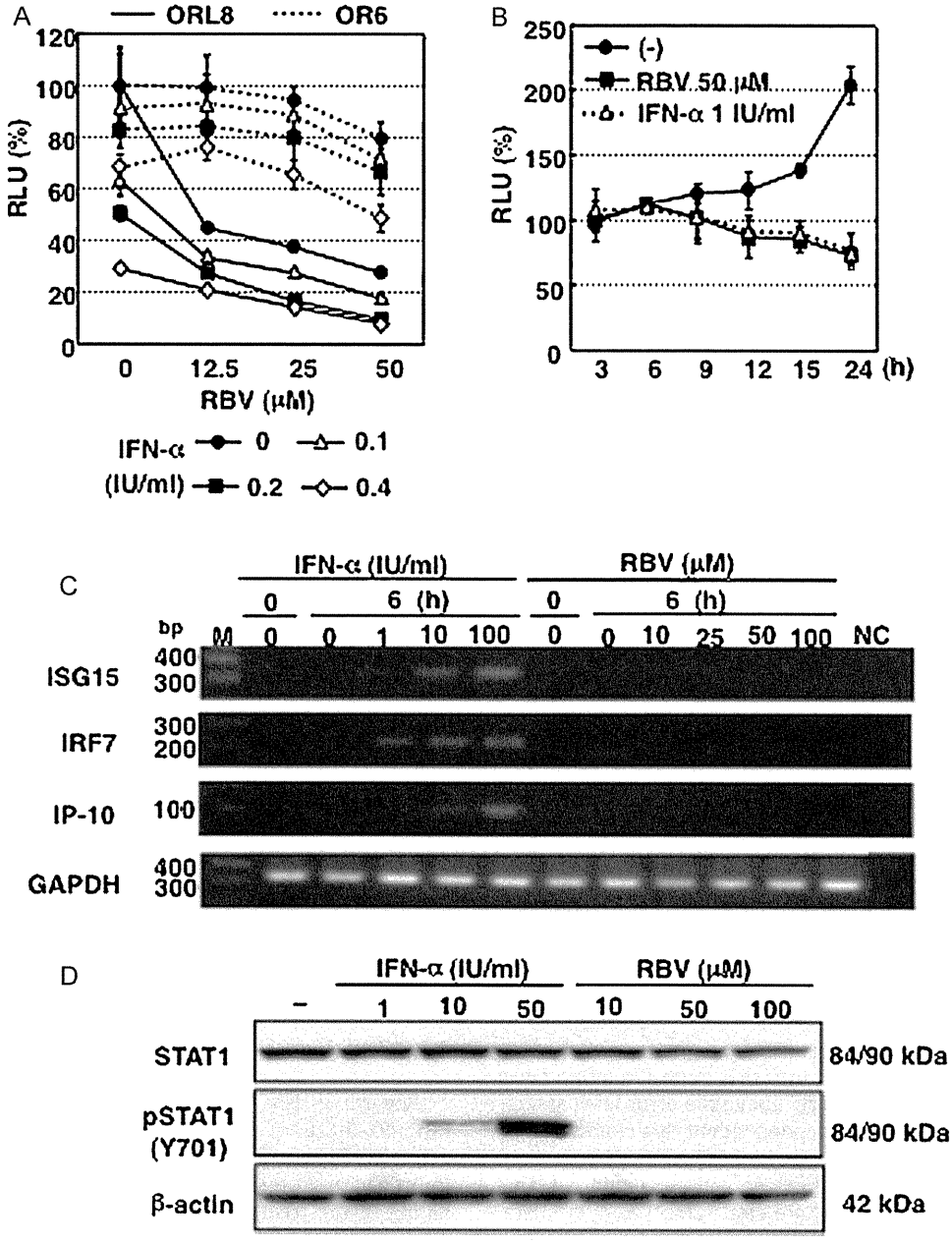

Fig. 4. RBV did not activate the IFN-signaling pathway in ORL8 cells. (A) Additive effect of RBV in combination with IFN-α. ORL8 and OR6 cells were treated with a combination of IFN-α and RBV for 72 h, after which the RL assay was performed. (B) Time course assay of the anti-HCV activity of RBV or IFN-α. ORL8 cells were treated with RBV or IFN-α, and an RL assay was performed at 3, 6, 9, 12, 15, and 24 h after treatment. Presented here is the RLU (%) calculated at each point, when the RL activity of non-treated cells at 3 h was assigned to be 100%. (C) ISGs were not induced by RBV treatment. ORL8 cells were treated with IFN-α or RBV for 6 h, and then the total RNAs extracted from the cells were subjected to RT-PCR using the primer sets for ISG15, IRF7, IP-10, and GAPDH as described in Section 2. RT-PCR products were detected by staining with ethidium bromide after 3% agarose gel electrophoresis. (D) Phosphorylation of STAT1 was not induced by RBV treatment. ORL8 cells were treated with IFN-α or RBV for 30 min, and subjected to Western blot analysis using anti-STAT1, anti-phospho-STAT1(Y701), and anti-β-actin antibodies.

tion in both assay systems, but its activity was greater in ORL8 than in OR6 (Fig. 4A). A comparative time course assay using RBV or IFN-α demonstrated that RBV- and IFN-α-treated ORL8 cells had the same anti-HCV kinetics, leading to decreased RL activity at 9 h after treatment (Fig. 4B). These results suggest that RBV induces some anti-HCV signaling pathway, such as an IFN-signaling pathway, rather than inducing IFN or directly inhibiting RNA replication.

We next examined the ability of RBV to activate ISGs. RT-PCR analysis revealed that RBV treatment (6 h) did not cause an induction of representative ISGs, ISG15, IRF7, and IP-10, in ORL8 cells, although even treatment (6 h) with 1 IU/ml (ISG15 and IRF7) or 10 IU/ml (IP-10) of IFN-α could induce these ISGs (Fig. 4C). Similar results were also obtained in OR6 cells and Huh7.5 cells (data not shown). In addition, enhancement of these ISGs was also not observed in the ORL8 cells co-treated with IFN-α and RBV (data not shown). Furthermore, we examined the phosphorylation status of STAT1 after RBV treatment. The results revealed that RBV treatment (up to 100 μM for 30 min) did not induce the phosphorylation of STAT1 in ORL8 cells, although phosphorylation of STAT1 was observed even after the treatment with 10 IU/ml of IFN-α (Fig. 4D). Together, these results indicate that RBV does not activate the IFN-signaling pathway.

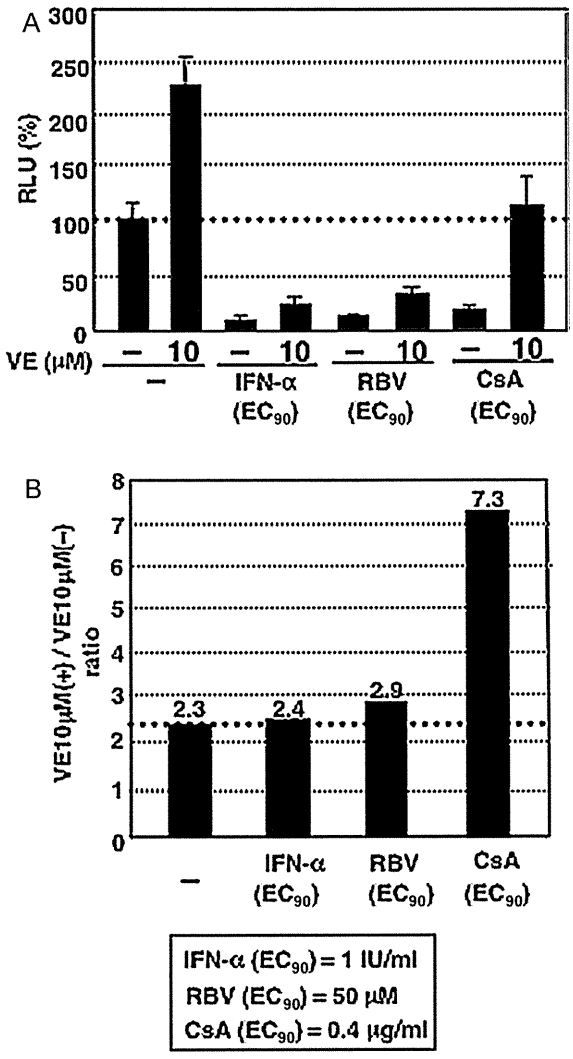

Fig. 5. The anti-HCV activity of RBV was not canceled by addition of VE. (A) Effects of VE on IFN-α, RBV, and CsA at the EC_{90}. ORL8 cells were treated with control medium (–), IFN-α, RBV, or CsA in either the absence or presence of VE for 72 h, and then an RL assay was performed. (B) The ratio of RL activity in the presence of VE to the RL activity in the absence of VE. The above ratio was calculated from the data of panel A. The horizontal line indicates the promotive effect of VE alone on HCV RNA replication as a baseline.

3.5. RBV did not induce the oxidative stress or subsequent anti-HCV status

Recently we reported that the antioxidant VE negated the antiviral activities of a broad range of anti-HCV reagents, including CsA, and demonstrated the involvement of the MEK-ERK1/2-signaling pathway in the anti-HCV status induced by oxidative stress (Yano et al., 2007, 2009). Therefore, we next expected that RBV induces oxidative stress. Accordingly, we examined the effect of VE on RBV, IFN-α, or CsA at the EC_{90} level in ORL8 system. Although the anti-HCV activity of CsA was canceled to a significant level by VE, the inhibitory effects of RBV and IFN-α were hardly influenced by co-treatment with VE (Fig. 5A). We normalized these results by dividing the RL value obtained in the presence of VE by that in the absence of VE as described previously (Yano et al., 2007) (Fig. 5B). The value of RBV was almost the same as that of IFN-α or control, although the value of CsA was somewhat higher (7.3) which was consistent with previous findings (Yano et al., 2007). These results suggest that induction of oxidative stress is not associated with the activity of RBV detected in ORL8 system.

3.6. Guanosine dose-dependently attenuated the anti-HCV activity of RBV

Previously, using a qualitative colony-forming efficiency (CFE) assay of an HCV RNA replicon, Zhou et al. (2003) showed that RBV (50 μM) reduced the CFE by 2-fold in HuH-7 cells, although 10 μM RBV did not result in a significant change in CFE. In that study, when exogenous guanosine, but not adenosine, which would replenish GTP pools via the salvage pathway, was co-administered with RBV, the RBV-induced CFE reduction was partially cancelled (Zhou et al., 2003). From this result, the authors suggested that IMPDH inhibition and subsequent lowering of GTP pools contribute to the observed reduction in CFE. However, they failed to observe the any suppressive effects of the IMPDH inhibitors MPA and Merimepodib (MMPD)/VX-497 on HCV RNA replication (Zhou et al., 2003). Conversely, Henry et al. showed that MPA exerted anti-HCV activity on HCV RNA replication in HuH-7-derived cells (Henry et al., 2006). Therefore, in order to resolve these controversial results, we initially examined the anti-HCV activity of MPA in ORL8 and OR6 systems. The results revealed that MPA strongly inhibited HCV RNA replication in both systems without suppression of cell growth. The EC_{50} values of MPA in the ORL8 and OR6 were 0.29 and 0.57 μM, respectively (Fig. 6A). Dose-dependent cancellation by guanosine, but not by adenosine, of the activity of MPA, was observed in both systems (Fig. 6B and data not shown for OR6 system). These results suggest that the depression of GTP induced by inhibition of IMPDH decreases the level of HCV RNA replication. From these results, we expected that anti-HCV activity of RBV observed in ORL8 might also have been associated with the inhibition of IMPDH. Indeed, significant dose-dependent cancellation by guanosine, but not by adenosine, of the anti-HCV activity of RBV (10 μM) was observed in ORL8 (Fig. 6C). ORL11 also showed a similar cancellation by guanosine (data not shown). The suppressive effect of guanosine on the activity of RBV in ORL8 was confirmed by Western blot analysis (Fig. 6D). These results suggest that the anti-HCV activity of RBV at clinically achievable concentrations in ORL8 is mediated through the inhibition of IMPDH by RBV.

3.7. IMPDH is required for HCV RNA replication

To confirm the involvement of IMPDH on HCV RNA replication, the endogenous expression of IMPDH was suppressed by siRNA specific to IMPDH. Since IMPDH has two isoforms, IMPDH1 and IMPDH2, which share 84% amino-acid homology (Wang et al., 2008), we prepared IMPDH1- and/or IMPDH2-knockdown ORL8 cells. The effective knockdown of IMPDH1 and/or IMPDH2 in ORL8 cells was confirmed by quantitative RT-PCR (Fig. 7A). We observed that the levels of HCV RNA replication in these knockdown cells were notably reduced compared with the control cells without suppression of cell growth (Fig. 7B). These results suggest that IMPDH is crucial for the maintenance of HCV RNA replication. Taken together, these results indicate that the inhibitory activity of RBV on HCV RNA replication in Li23-derived cells is mediated through the inhibition of IMPDH by RBV.

4. Discussion

In this study, using novel Li23-derived cell culture assay systems, we demonstrated for the first time that RBV at clinically achievable concentrations efficiently inhibited HCV RNA replication, and clarified that its anti-HCV activity was mediated by the inhibition of IMPDH.

To date, several mechanisms as described above have been proposed based on the results of studies using an HuH-7-derived cell culture system (Feld and Hoofnagle, 2005; Feld et al., 2010; Lau

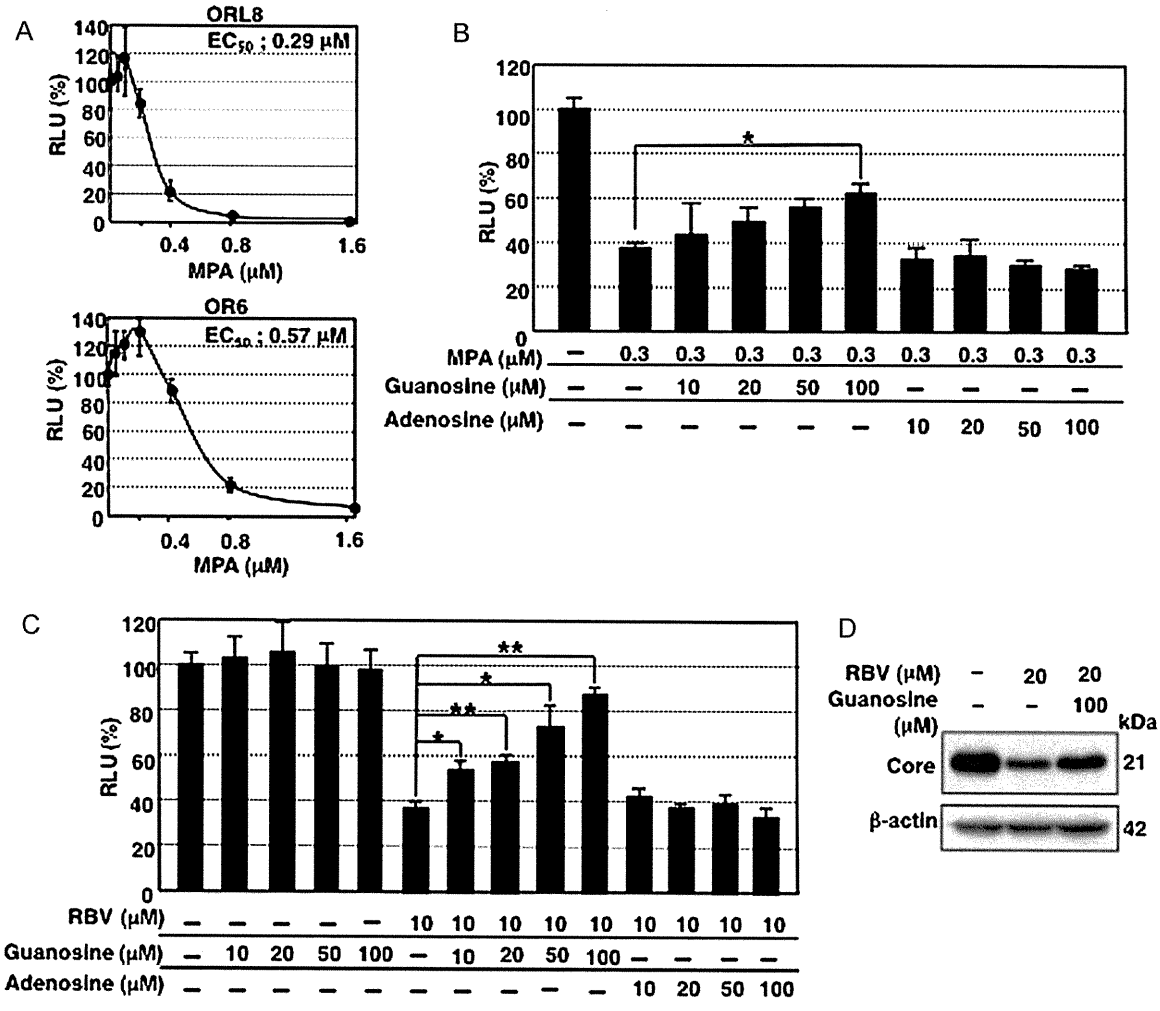

Fig. 6. Guanosine canceled the anti-HCV activity of RBV in ORL8 system. (A) Anti-HCV activity of MPA in ORL8 and OR6. The ORL8 and OR6 cells were treated with MPA for 72 h, and then RL assay was performed. (B) Effect of guanosine or adenosine on MPA in ORL8 system. ORL8 cells were treated with MPA alone or in combination with guanosine or adenosine for 72 h, and then RL assay was performed. Asterisk indicates a significant difference compared to the control treatment. *$P < 0.05$. (C) Effect of guanosine or adenosine on RBV in ORL8 system. ORL8 cells were treated with RBV alone or in combination with guanosine or adenosine for 72 h, and then the RL assay was performed. Asterisks indicate significant differences compared to the control treatment. *$P < 0.05$; **$P < 0.01$. (D) Effect of guanosine on RBV in ORL8 system. ORL8 cells were treated with RBV alone or in combination with guanosine for 72 h, and subjected to Western blot analysis using anti-Core and β-actin antibodies.

et al., 2002; Thomas et al., 2011; Zhou et al., 2003). Although the effective concentrations (50–1000 μM) of RBV in those studies were much higher than the clinically achievable concentrations (5–14 μM) (Feld et al., 2010; Pawlotsky et al., 2004; Tanabe et al., 2004), the effective concentration of RBV in this study was close to the clinically achievable concentrations. Furthermore, it is noteworthy that the replication of a different HCV strain (JFH1 of genotype 2a) in the Li23-derived cell culture system, but not in the HuH-7-derived cell culture system, was also suppressed with RBV at the concentration of 10 μM (Fig. 1C). These results demonstrate that the Li23 cell-derived assay system is a more sensitive biosensor of RBV than the HuH-7 cell-derived assay system.

The finding that RBV remarkably inhibited HCV RNA replication in our new assay systems led us to analyze the anti-HCV mechanism of RBV. In this study, we evaluated several possible anti-HCV mechanisms of RBV, as described above. Regarding the induction of error catastrophe by RBV, we obtained no evidence that RBV (even at 50 μM) acted as a mutagen in HCV RNA replication. Therefore, we could not explain the mechanism underlying the suppression of HCV RNA replication by RBV according to the theory of error catastrophe. In addition, no increasing mutation rate of HCV RNA in patients receiving RBV monotherapy or a combination of RBV plus IFN-α was observed in a previous clinical study (Chevaliez and Pawlotsky, 2007). In consideration of all these findings, we suggest that the clinically achievable concentrations of RBV do not act as a mutagen in HCV RNA replication. Indeed, our previous study using the replicon cell culture system demonstrated that RBV treatment (6 months at 5 and 25 μM) did not accelerate the mutation rate or increase the genetic diversity of the HCV replicon (Kato et al., 2005). In regard to the effect of RBV on the IFN system, we obtained no evidence that RBV (even at 50 μM) induced ISGs (ISG15, IRF7, and IP-10) or phosphorylation of STAT1 even in the cells co-treated with IFN-α and RBV (data not shown). On the other hand, very recently Thomas et al. (Thomas et al., 2011) reported that RBV treatment (500 μM) resulted in the induction of a distinct set of ISGs including ISG15, IRF7, and IRF9, using HuH-7-derived cell line Huh7.5.1. In that study, they demonstrated that the induction of these ISGs was mediated by a novel mechanism different from those associated with IFN signaling and double stranded RNA sensing pathway, and concluded that the effect of RBV on ISG regulation is IFN-independent. However, in our cell culture system, which is highly sensitive to RBV, the induction of ISG15 and IRF7 by RBV was not observed (Fig. 4C). This kind of controversial results may be dependent on the difference of cell lines used in both studies, since recent microarray analysis revealed that the expression profiles of Li23 and HuH-7 cells, both of which possess an environment

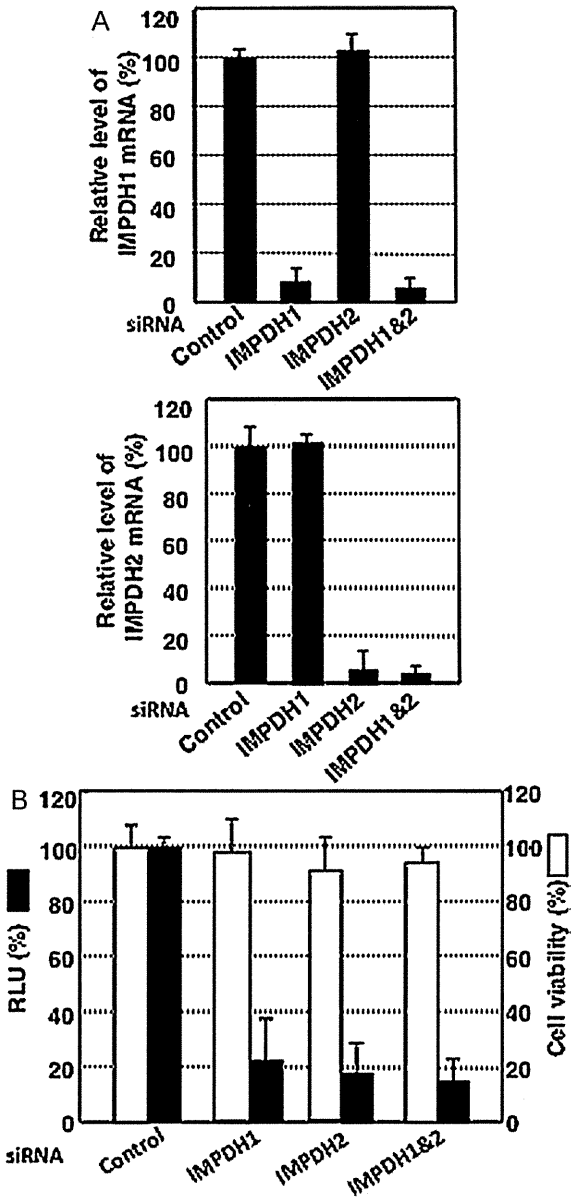

Fig. 7. IMPDH is required for HCV RNA replication. (A) Inhibition of IMPDH1 and IMPDH2 expression by siRNA in ORL8 cells. ORL8 cells were transfected with 8 nM siRNA targeting for IMPDH1 and/or IMPDH2. After 72 h, the expression levels of IMPDH1 and IMPDH2 mRNAs were determined by the quantitative RT-PCR. Experiments were done in triplicate. (B) Suppression of HCV RNA replication in IMPDH1- and/or IMPDH2-knockdown ORL8 cells. The RLU (%) calculated, when the luciferase activity of the cells treated with control siRNA was assigned to be 100%, is shown. The cell viability was determined as described in Section 2.

for robust HCV replication, differed considerably (Kato et al., 2009; Mori et al., 2010). However, Thomas et al. (2011) observed that the addition of guanosine to the medium could block RBV-induced ISGs induction. Therefore, further additional studies would be needed to resolve the differences of results obtained from both studies.

The highlight in this study is that a Li23-derived cell culture system clearly demonstrated an association between the suppression of HCV RNA replication by RBV and IMPDH inhibition by RBV. Although RBV is known to be an IMPDH inhibitor (Lau et al., 2002), it had been considered that such inhibitory activity would not contribute to the anti-HCV activity of RBV, because of the marginal antiviral effect of RBV in HuH-7-derived HCV RNA replicating cells (Naka et al., 2005; Tanabe et al., 2004; Zhou et al., 2003). Although Zhou et al. (2003) previously showed that exogenous guanosine cancelled the RBV-induced CFE reduction using an HuH-7-based HCV replicon system, they did not observe any dose-dependent reversion of the adverse effect of RBV by the addition of guanosine. However, in our Li23-based HCV replication assay system, we observed a near complete cancellation of the activity of RBV in the dose-dependent manner of guanosine (Fig. 6C). This finding indicated that anti-HCV activity of RBV might be mediated through the inhibition of IMPDH by RBV. Indeed, we could demonstrate that HCV RNA replication was notably suppressed in IMPDH-knockdown ORL8 cells (Fig. 7B). Taken together, these results revealed that the Li23-derived assay system was superior to HuH-7-derived assay system in order to clarify the anti-HCV mechanism of RBV.

The remarkable effect of RBV observed in this study was considered to be due to the difference in the cell lines used, because Li23-derived cells possessed rather different gene expression profiles from those in HuH-7-derived cells (Kato et al., 2009; Mori et al., 2010). As one of the possibilities, we examined the expression status of nucleoside transporters (ENT family) involved in cellular uptake of RBV or ATP-binding cassette transporters, including multidrug resistance 1, which is involved in cellular excretion. However, the mRNA levels of these transporters were almost the same in both types of cells (Fig. 3C). Although unfortunately we failed to clarify the mechanism underlying the remarkable differences in the activity of RBV in both types of cells, we observed that the anti-HCV activity of RBV was completely canceled by NBMPR, an ENT inhibitor, suggesting that RBV is taken by ENT member(s) at least in ORL8 cells. This finding supports the recent report describing the involvement of ENT1 on cellular uptake of RBV (Fukuchi et al., 2010; Ibarra and Pfeiffer, 2009). Therefore, a comparative analysis regarding the functions of ENT member(s) derived from both types of cells will be needed. As the other possibility, the differences of activities or expression levels of IMPDH in OR6 and ORL8 cells may contribute to the remarkable effect of RBV observed in ORL8 cells.

On the other hand, it has been known that rapid reduction of the intracellular level of GTP occurs when RBV inhibits IMPDH (Feld and Hoofnagle, 2005). Therefore, it is assumed that the decrease of GTP would lead to a suppression of HCV replication. To date, several studies (Lohmann et al., 1999; Luo et al., 2000; Simister et al., 2009) have shown that high concentration of GTP (approximately 500 μM corresponding to the intracellular concentration) is required for the efficient de novo initiation of RNA synthesis by HCV NS5B RdRp. In addition, Simister et al. (2009) showed that change from 500 μM to 100 μM of GTP concentration decreased a log of the NS5B RdRp activity. From these studies, we expect that the inhibition of IMPDH by RBV may cause rapid decrease of intracellular GTP concentration, resulting in the suppression of de novo RNA synthesis by NS5B. Before our assumption, MMPD/VX-497 has developed as an inhibitor of IMPDH, and it has been shown to exert anti-HCV activity (EC_{50}; 0.39 μM) in an HCV replicon system (Marcellin et al., 2007). However, MMPD/VX-497 monotherapy of patients with chronic hepatitis C had no effect on HCV RNA levels (Marcellin et al., 2007) just as, in another study, RBV monotherapy had no effect on HCV RNA levels in patients with chronic hepatitis C (Di Bisceglie et al., 1995). Although we showed that the EC_{50} value of RBV in this study was equivalent to the clinically achievable concentrations (Feld et al., 2010; Pawlotsky et al., 2004; Tanabe et al., 2004), we considered that the effective concentration for a reduction of HCV RNA levels in monotherapy would be less than the EC_{90} value. However, an IMPDH inhibitor at EC_{50} would be effective in combination with IFN-α as an adjuvant. Indeed, combination therapy with IFN-α and MMPD/VX-497 was effective in previously untreated patients with chronic hepatitis C (McHutchison et al., 2005). However, a recent study (Rustgi et al., 2009) showed that the addition of MMPD/VX-497 to PEG-IFN-α and RBV combination

therapy in patients who had been nonrespondent to PEG-IFN-α and RBV combination therapy did not increase the proportion of patients who achieved an SVR. Since we showed that RBV also acted as an IMPDH inhibitor in the present study, it would seem to be a reasonable result that MMPD/VX-497 had no significant effect on patients who were nonresponsive to combination therapy with PEG-IFN-α and RBV.

In conclusion, we clarified the anti-HCV mechanism of RBV in a new HCV cell culture system. The fact that anti-HCV activity of RBV was mediated by the inhibition of IMPDH would provide a clue to the mechanism of the increase of SVR by the current standard combination therapy with PEG-IFN-α and RBV. In addition, our findings should also be useful for the screening and development of new anti-HCV drugs, which inhibit IMPDH, with reduced side effects, including anemia.

Acknowledgments

We would like to thank Naoko Kawahara, Takashi Nakamura, and Keiko Takeshita for their technical assistances. This work was supported by a grant-in-aid for research on hepatitis from the Ministry of Health, Labor, and Welfare of Japan. K. M. was supported by a Research Fellowship from the Japan Society for Promotion of Science for Young Scientists.

References

Ariumi, Y., Kuroki, M., Abe, K., Dansako, H., Ikeda, M., Wakita, T., Kato, N., 2007. DDX3 DEAD-box RNA helicase is required for hepatitis C virus RNA replication. J. Virol. 81, 13922–13926.

Chevaliez, S., Brillet, R., Lázaro, E., Hézode, C., Pawlotsky, J.M., 2007. Analysis of ribavirin mutagenicity in human hepatitis C virus infection. J. Virol. 81, 7732–7741.

Chevaliez, S., Pawlotsky, J.M., 2007. Interferon-based therapy of hepatitis C. Adv. Drug. Deliv. Rev. 59, 1222–1241.

Contreras, A.M., Hiasa, Y., He, W., Terella, A., Schmidt, E.V., Chung, R.T., 2002. Viral RNA mutations are region specific and increased by ribavirin in a full-length hepatitis C virus replication system. J. Virol. 76, 8505–8517.

Dansako, H., Ikeda, M., Kato, N., 2007. Limited suppression of the interferon-beta production by hepatitis C virus serine protease in cultured human hepatocytes. FEBS J. 274, 4161–4176.

Dansako, H., Naganuma, A., Nakamura, T., Ikeda, F., Nozaki, A., Kato, N., 2003. Differential activation of interferon-inducible genes by hepatitis C virus core protein mediated by the interferon stimulated response element. Virus Res. 97, 17–30.

Di Bisceglie, A.M., Conjeevaram, H.S., Fried, M.W., Sallie, R., Park, Y., Yurdaydin, C., Swain, M., Kleiner, D.E., Mahaney, K., Hoofnagle, J.H., 1995. Ribavirin as therapy for chronic hepatitis C. A randomized, double-blind, placebo-controlled trial. Ann. Intern. Med. 123, 897–903.

Feld, J.J., Lutchman, G.A., Heller, T., Hara, K., Pfeiffer, J.K., Leff, R.D., Meek, C., Rivera, M., Ko, M., Koh, C., Rotman, Y., Ghany, M.G., Haynes-Williams, V., Neumann, A.U., Liang, T.J., Hoofnagle, J.H., 2010. Ribavirin improves early responses to peginterferon through improved interferon signaling. Gastroenterology 139, 154–162.

Feld, J.J., Hoofnagle, J.H., 2005. Mechanism of action of interferon and ribavirin in treatment of hepatitis C. Nature 436, 967–972.

Fukuchi, Y., Furihata, T., Hashizume, M., Iikura, M., Chiba, K., 2010. Characterization of ribavirin uptake systems in human hepatocytes. J. Hepatol. 52, 486–492.

Henry, S.D., Metselaar, H.J., Lonsdale, R.C., Kok, A., Haagmans, B.L., Tilanus, H.W., van der Laan, L.J., 2006. Mycophenolic acid inhibits hepatitis C virus replication and acts in synergy with cyclosporin A and interferon-alpha. Gastroenterology 131, 1452–1462.

Ibarra, K.D., Pfeiffer, J.K., 2009. Reduced ribavirin antiviral efficacy via nucleoside transporter-mediated drug resistance. J. Virol. 83, 4538–4547.

Ikeda, M., Abe, K., Dansako, H., Nakamura, T., Naka, K., Kato, N., 2005. Efficient replication of a full-length hepatitis C virus genome, strain O, in cell culture, and development of a luciferase reporter system. Biochem. Biophys. Res. Commun. 329, 1350–1359.

Kato, N., Hijikata, M., Ootsuyama, Y., Nakagawa, M., Ohkoshi, S., Sugimura, T., Shimotohno, K., 1990. Molecular cloning of the human hepatitis C virus genome from Japanese patients with non-A, non-B hepatitis. Proc. Natl. Acad. Sci. U.S.A. 87, 9524–9528.

Kato, N., Mori, K., Abe, K., Dansako, H., Kuroki, M., Ariumi, Y., Wakita, T., Ikeda, M., 2009. Efficient replication systems for hepatitis C virus using a new human hepatoma cell line. Virus Res. 146, 41–50.

Kato, N., Nakamura, T., Dansako, H., Namba, K., Abe, K., Nozaki, A., Naka, K., Ikeda, M., Shimotohno, K., 2005. Genetic variation and dynamics of hepatitis C virus replicons in long-term cell culture. J. Gen. Virol. 86, 645–656.

Kato, N., Sugiyama, K., Namba, K., Dansako, H., Nakamura, T., Takami, M., Naka, K., Nozaki, A., Shimotohno, K., 2003. Establishment of a hepatitis C virus subgenomic replicon derived from human hepatocytes infected in vitro. Biochem. Biophys. Res. Commun. 306, 756–766.

Lau, J.Y., Tam, R.C., Liang, T.J., Hong, Z., 2002. Mechanism of action of ribavirin in the combination treatment of chronic HCV infection. Hepatology 35, 1002–1009.

Liu, W.L., Su, W.C., Cheng, C.W., Hwang, L.H., Wang, C.C., Chen, H.L., Chen, D.S., Lai, M.Y., 2007. Ribavirin up-regulates the activity of double-stranded RNA-activated protein kinase and enhances the action of interferon-alpha against hepatitis C virus. J. Infect. Dis. 196, 425–434.

Lohmann, V., Overton, H., Bartenschlager, R., 1999. Selective stimulation of hepatitis C virus and pestivirus NS5B RNA polymerase activity by GTP. J. Biol. Chem. 274, 10807–10815.

Luo, G., Hamatake, R.K., Mathis, D.M., Racela, J., Rigat, K.L., Lemm, J., Colonno, R.J., 2000. De novo initiation of RNA synthesis by the RNA-dependent RNA polymerase (NS5B) of hepatitis C virus. J. Virol. 74, 851–863.

Marcellin, P., Horsmans, Y., Nevens, F., Grange, J.D., Bronowicki, J.P., Vetter, D., Purdy, S., Garg, V., Bengtsson, L., McNair, L., Alam, J., 2007. Phase 2 study of the combination of merimepodib with peginterferon-alpha2b, and ribavirin in nonresponders to previous therapy for chronic hepatitis C. J. Hepatol. 47, 476–483.

McHutchison, J.G., Shiffman, M.L., Cheung, R.C., Gordon, S.C., Wright Jr., T.L., Pottage, J.C., McNair, L., Ette, E., Moseley, S., Alam, J., 2005. A randomized, double-blind, placebo-controlled dose-escalation trial of merimepodib (VX-497) and interferon-alpha in previously untreated patients with chronic hepatitis C. Antivir. Ther. 10, 635–643.

Mori, K., Ikeda, M., Ariumi, Y., Kato, N., 2010. Gene expression profile of Li23, a new human hepatoma cell line that enables robust hepatitis C virus replication, Comparison with HuH-7 and other hepatic cell lines. Hepatol. Res. 40, 1248–1253.

Naka, K., Ikeda, M., Abe, K., Dansako, H., Kato, N., 2005. Mizoribine inhibits hepatitis C virus RNA replication, effect of combination with interferon-alpha. Biochem. Biophys. Res. Commun. 330, 871–879.

Pastor-Anglada, M., Cano-Soldado, P., Molina-Arcas, M., Lostao, M.P., Larráyoz, I., Martínez-Picado, J., Casado, F.J., 2005. Cell entry and export of nucleoside analogues. Virus Res. 107, 151–164.

Pawlotsky, J.M., Dahari, H., Neumann, A.U., Hezode, C., Germanidis, G., Lonjon, I., Castera, L., Dhumeaux, D., 2004. Antiviral action of ribavirin in chronic hepatitis C. Gastroenterology 126, 703–714.

Rustgi, V.K., Lee, W.M., Lawitz, E., Gordon, S.C., Afdhal, N., Poordad, F., Bonkovsky, H.L., Bengtsson, L., Chandorkar, G., Harding, M., McNair, L., Aalyson, M., Alam, J., Kauffman, R., Gharakhanian, S., McHutchison, J.G., MErimepodib TRiple cOmbination Study Group, 2009. Merimepodib, pegylated interferon, and ribavirin in genotype 1 chronic hepatitis C pegylated interferon and ribavirin nonresponders. Hepatology 50, 1719–1726.

Simister, P., Schmitt, M., Geitmann, M., Wicht, O., Danielson, U.H., Klein, R., Bressanelli, S., Lohmann, V., 2009. Structural and functional analysis of hepatitis C virus strain JFH1 polymerase. J. Virol. 83, 11926–11939.

Tanabe, Y., Sakamoto, N., Enomoto, N., Kurosaki, M., Ueda, E., Maekawa, S., Yamashiro, T., Nakagawa, M., Chen, C.H., Kanazawa, N., Kakinuma, S., Watanabe, M., 2004. Synergistic inhibition of intracellular hepatitis C virus replication by combination of ribavirin and interferon-alpha. J. Infect. Dis. 189, 1129–1139.

Thomas, D.L., 2000. Hepatitis C epidemiology. Curr. Top. Microbial. Immunol. 242, 25–41.

Thomas, E., Feld, J.J., Li, Q., Hu, Z., Fried, M.W., Liang, T.J., 2011. Ribavirin potentiates interferon action by augmenting interferon-stimulated gene induction in HCV cell culture models. Hepatology 53, 32–41.

Wakita, T., Pietschmann, T., Kato, T., Date, T., Miyamoto, M., Zhao, Z., Murthy, K., Habermann, A., Kräusslich, H.G., Mizokami, M., Bartenschlager, R., Liang, T.J., 2005. Production of infectious hepatitis C virus in tissue culture from a cloned viral genome. Nat. Med. 11, 791–796.

Wang, J., Yang, J.W., Zeevi, A., Webber, S.A., Girnita, D.M., Selby, R., Fu, J., Shah, T., Pravica, V., Hutchinson, I.V., Burckart, G.J., 2008. IMPDH1 gene polymorphisms and association with acute rejection in renal transplant patients. Clin. Pharmacol. Ther. 83, 711–717.

Yano, M., Ikeda, M., Abe, K., Dansako, H., Ohkoshi, S., Aoyagi, Y., Kato, N., 2007. Comprehensive analysis of the effects of ordinary nutrients on hepatitis C virus RNA replication in cell culture. Antimicrob. Agents Chemother. 51, 2016–2127.

Yano, M., Ikeda, M., Abe, K., Kawai, Y., Kuroki, M., Mori, K., Dansako, H., Ariumi, Y., Ohkoshi, S., Aoyagi, Y., Kato, N., 2009. Oxidative stress induces anti-hepatitis C virus status via the activation of extracellular signal-regulated kinase. Hepatology 50, 678–688.

Zhou, S., Liu, R., Baroudy, B.M., Malcolm, B.A., Reyes, G.R., 2003. The effect of ribavirin and IMPDH inhibitors on hepatitis C virus subgenomic replicon RNA. Virology 310, 333–342.

JOURNAL OF VIROLOGY, July 2011, p. 6882–6892 Vol. 85, No. 14
0022-538X/11/$12.00 doi:10.1128/JVI.02418-10

Hepatitis C Virus Hijacks P-Body and Stress Granule Components around Lipid Droplets[▽]

Yasuo Ariumi,[1,2]* Misao Kuroki,[1] Yukihiro Kushima,[3] Kanae Osugi,[4] Makoto Hijikata,[3] Masatoshi Maki,[4] Masanori Ikeda,[1] and Nobuyuki Kato[1]

Department of Tumor Virology, Okayama University Graduate School of Medicine, Dentistry, and Pharmaceutical Sciences, Okayama 700-8558, Japan[1]; Center for AIDS Research, Kumamoto University, Kumamoto 860-0811, Japan[2]; Department of Viral Oncology, Institute for Virus Research, Kyoto University, Kyoto 606-8507, Japan[3]; and Department of Applied Molecular Biosciences, Graduate School of Bioagricultural Sciences, Nagoya University, Nagoya 464-8601, Japan[4]

Received 19 November 2010/Accepted 21 April 2011

The microRNA miR-122 and DDX6/Rck/p54, a microRNA effector, have been implicated in hepatitis C virus (HCV) replication. In this study, we demonstrated for the first time that HCV-JFH1 infection disrupted processing (P)-body formation of the microRNA effectors DDX6, Lsm1, Xrn1, PATL1, and Ago2, but not the decapping enzyme DCP2, and dynamically redistributed these microRNA effectors to the HCV production factory around lipid droplets in HuH-7-derived RSc cells. Notably, HCV-JFH1 infection also redistributed the stress granule components GTPase-activating protein (SH3 domain)-binding protein 1 (G3BP1), ataxin-2 (ATX2), and poly(A)-binding protein 1 (PABP1) to the HCV production factory. In this regard, we found that the P-body formation of DDX6 began to be disrupted at 36 h postinfection. Consistently, G3BP1 transiently formed stress granules at 36 h postinfection. We then observed the ringlike formation of DDX6 or G3BP1 and colocalization with HCV core after 48 h postinfection, suggesting that the disruption of P-body formation and the hijacking of P-body and stress granule components occur at a late step of HCV infection. Furthermore, HCV infection could suppress stress granule formation in response to heat shock or treatment with arsenite. Importantly, we demonstrate that the accumulation of HCV RNA was significantly suppressed in DDX6, Lsm1, ATX2, and PABP1 knockdown cells after the inoculation of HCV-JFH1, suggesting that the P-body and the stress granule components are required for the HCV life cycle. Altogether, HCV seems to hijack the P-body and the stress granule components for HCV replication.

Hepatitis C virus (HCV) is the causative agent of chronic hepatitis, which progresses to liver cirrhosis and hepatocellular carcinoma. HCV is an enveloped virus with a positive single-stranded 9.6-kb RNA genome, which encodes a large polyprotein precursor of approximately 3,000 amino acid (aa) residues. This polyprotein is cleaved by a combination of the host and viral proteases into at least 10 proteins in the following order: core, envelope 1 (E1), E2, p7, nonstructural 2 (NS2), NS3, NS4A, NS4B, NS5A, and NS5B (12, 13, 21). The HCV core protein, a nucleocapsid, is targeted to lipid droplets (LDs), and the dimerization of the core protein by a disulfide bond is essential for the production of infectious virus (24). Recently, LDs have been found to be involved in an important cytoplasmic organelle for HCV production (26). Budding is an essential step in the life cycle of enveloped viruses. The endosomal sorting complex required for transport (ESCRT) system has been involved in such enveloped virus budding machineries, including that of HCV (5).

DEAD-box RNA helicases with ATP-dependent RNA-unwinding activities have been implicated in various RNA metabolic processes, including transcription, translation, RNA splicing, RNA transport, and RNA degradation (32). Previously, DDX3 was identified as an HCV core-interacting protein by yeast two-hybrid screening (25, 29, 43). Indeed, DDX3 is required for HCV RNA replication (3, 31). DDX6 (Rck/p54) is also required for HCV replication (16, 33). DDX6 interacts with an initiation factor, eukaryotic initiation factor 4E (eIF-4E), to repress the translational activity of mRNP (38). Furthermore, DDX6 regulates the activity of the decapping enzymes DCP1 and DCP2 and interacts directly with Argonaute-1 (Ago1) and Ago2 in the microRNA (miRNA)-induced silencing complex (miRISC) and is involved in RNA silencing. DDX6 localizes predominantly in the discrete cytoplasmic foci termed the processing (P) body. Thus, the P body seems to be an aggregate of translationally repressed mRNPs associated with the translation repression and mRNA decay machinery.

In addition to the P body, eukaryotic cells contain another type of RNA granule termed the stress granule (SG) (1, 6, 22, 30). SGs are aggregates of untranslating mRNAs in conjunction with a subset of translation initiation factors (eIF4E, eIF3, eIF4A, eIFG, and poly(A)-binding protein [PABP]), the 40S ribosomal subunits, and several RNA-binding proteins, including PABP, T cell intracellular antigen 1 (TIA-1), TIA-1-related protein (TIAR), and GTPase-activating protein (SH3 domain)-binding protein 1 (G3BP1). SGs regulate mRNA translation and decay as well as proteins involved in various aspects of mRNA metabolisms. SGs are cytoplasmic phase-dense structures that occur in eukaryotic cells exposed to various environmental stress, including heat, arsenite, viral infection, oxidative conditions, UV irradiation, and hypoxia. Impor-

* Corresponding author. Mailing address: Center for AIDS Research, Kumamoto University, 2-2-1 Honjo, Kumamoto 860-0811, Japan. Phone and fax: 81 96 373 6834. E-mail: ariumi@kumamoto-u.ac.jp.
▽ Published ahead of print on 4 May 2011.

tantly, several viruses target SGs and stress granule components for viral replication (10, 11, 34, 39). Recent studies suggest that SGs and the P body physically interact and that mRNAs may move between the two compartments (1, 6, 22, 28, 30).

miRNAs are a class of small noncoding RNA molecules ~21 to 22 nucleotides (nt) in length. miRNAs usually interact with 3′-untranslated regions (UTRs) of target mRNAs, leading to the downregulation of mRNA expression. Notably, the liver-specific and abundant miR-122 interacts with the 5′-UTR of the HCV RNA genome and facilitates HCV replication (15, 17, 19, 20, 31). Ago2 is at least required for the efficient miR-122 regulation of HCV RNA accumulation and translation (40). However, the molecular mechanism(s) for how DDX6 and miR-122 as well as DDX3 positively regulate HCV replication is not fully understood. Therefore, we investigated the potential role of P-body and stress granule components in HCV replication.

MATERIALS AND METHODS

Cell culture. 293FT cells were cultured in Dulbecco's modified Eagle's medium (DMEM; Invitrogen, Carlsbad, CA) supplemented with 10% fetal bovine serum (FBS). HuH-7-derived RSc cured cells, in which cell culture-generated HCV-JFH1 (JFH1 strain of genotype 2a) (37) could infect and effectively replicate, were cultured in DMEM with 10% FBS as described previously (3–5, 23).

Plasmid construction. To construct pcDNA3-FLAG-DDX6, a DNA fragment encoding DDX6 was amplified from total RNAs derived from RSc cells by reverse transcription (RT)-PCR using KOD-Plus DNA polymerase (Toyobo) and the following pairs of primers: 5′-CGGGATCCAAGATGAGCACGGCC AGAACAGAGAACCCTGTT-3′ (forward) and 5′-CCGCTCGAGTTAAGGT TTCTCATCTTCTACAGGCTCGCT-3′ (reverse). The obtained DNA fragments were subcloned into either BamHI-XhoI site of the pcDNA3-FLAG vector (2), and the nucleotide sequences were determined by BigDye termination cycle sequencing using an ABI Prism 310 genetic analyzer (Applied Biosystems, Foster City, CA).

RNA interference. The following small interfering RNAs (siRNAs) were used: human ATXN2/ATX2/ataxin-2 (siGENOME SMRT pool M-011772-01-005), human PABP1/PABPC1 (siGENOME SMRT pool M-019598-01-005), human Lsm1 (siGENOME SMRT pool M-005124-01-005), human Xrn1 (siGENOME SMRT pool M-013754-01-005), human G3BP1 (ON-TARGETplus SMRT pool L-012099-00-005), human PATL1 (siGENOME SMRT pool M-015591-00-005), and siGENOME nontargeting siRNA pool 1 (D-001206-13-05) (Dharmacon, Thermo Fisher Scientific, Waltham, MA), as a control. siRNAs (25 nM final concentration) were transiently transfected into RSc cells (3–5, 23) using Oligofectamine (Invitrogen) according to the manufacturer's instructions. Oligonucleotides with the following sense and antisense sequences were used for the cloning of short hairpin RNA (shRNA)-encoding sequences targeted to DDX6 (DDX6i) as well as the control nontargeting shRNA (shCon) in a lentiviral vector: 5′-GATCC CCGGAGGAACTAACTCTGAAGTTCAAGAGACTTCAGAGTTAGTTCCT CCTTTTTGGAAA-3′ (sense) and 5′-AGCTTTTCCAAAAAGGAGGAACTAA CTCTGAAGTCTCTTGAACTTCAGAGTTAGTTCCTCCGGG-3′ (antisense) for DDX6i and 5′-GATCCCCGAATCCAGAGGTAATCTACTTCAAGAGA GTAGATTACCTCTGGATTCTTTTTGGAAA-3′ (sense) and 5′-AGCTTTTC CAAAAAGAATCCAGAGGTAATCTACTCTCTTGAAGTAGATTACCTC TGGATTCGGG-3′ (antisense) for shCon. The oligonucleotides described above were annealed and subcloned into the BglII-HindIII site, downstream from an RNA polymerase III promoter of pSUPER (8), to generate pSUPER-DDX6i and pSUPER-shCon, respectively. To construct pLV-DDX6i and pLV-shCon, the BamHI-SalI fragments of the corresponding pSUPER plasmids were subcloned into the BamHI-SalI site of pRDI292, an HIV-1-derived self-inactivating lentiviral vector containing a puromycin resistance marker allowing for the selection of transduced cells (7). pLV-DDX3i, described previously (3), was used.

Lentiviral vector production. The vesicular stomatitis virus G protein (VSV-G)-pseudotyped HIV-1-based vector system was described previously (27, 44). The lentiviral vector particles were produced by the transient transfection of the second-generation packaging construct pCMV-ΔR8.91 (27, 44), the VSV-G-envelope-expressing plasmid pMDG2, as well as pRDI292 into 293FT cells with FuGene6 reagent (Roche Diagnostics, Mannheim, Germany).

HCV infection experiments. The supernatants were collected from cell culture-generated HCV-JFH1 (37)-infected RSc cells (3–5, 23) at 5 days postinfection and stored at −80°C after filtering through a 0.45-μm filter (Kurabo, Osaka, Japan) until use. For infection experiments with HCV-JFH1, RSc cells (1×10^5 cells/well) were plated onto 6-well plates and cultured for 24 h. We then infected the cells at a multiplicity of infection (MOI) of 1 or 4. The culture supernatants were collected at 24 h postinfection, and the levels of the core protein were determined by an enzyme-linked immunosorbent assay (ELISA) (Mitsubishi Kagaku Bio-Clinical Laboratories, Tokyo, Japan). Total RNA was also isolated from the infected cellular lysates by using an RNeasy minikit (Qiagen, Hilden, Germany) for analysis of intracellular HCV RNA. The infectivity of HCV-JFH1 in the culture supernatants was determined by a focus-forming assay at 48 h postinfection. HCV-JFH1-infected cells were detected by using anti-HCV core (CP-9 and CP-11 mixture).

Quantitative RT-PCR analysis. The quantitative RT-PCR analysis of HCV RNA was performed by real-time LightCycler PCR (Roche) as described previously (3–5, 14, 23). We used the following forward and reverse primer sets for the real-time LightCycler PCR: 5′-ATGAGTCATGTGGCAGTGGA-3′ (forward) and 5′-GCTGGCTGTACTTCCTCCAC-3′ (reverse) for DDX3, 5′-ATG AGCACGGCCAGAACAGA-3′ (forward) and 5′-TTGCTGTGTCTGTGTGC CCC-3′ (reverse) for DDX6, 5′-TGACGGGGTCACCCACACTG-3′ (forward) and 5′-AAGCTGTAGCCGCGCTCGGT-3′ (reverse) for β-actin, and 5′-AGA GCCATAGTGGTCTGCGG-3′ (forward) and 5′-CTTTCGCAACCCAACGC TAC-3′ (reverse) for HCV-JFH1.

Preparation of anti-PATL1 antibody. The anti-PATL1 antiserum was raised in rabbits using the glutathione *S*-transferase (GST)-fused PATL1 Ct (C-terminal region of PATL1, aa 450 to 770) as an antigen, and immunoglobulins were affinity purified by using the maltose-binding protein (MBP)-fused PATL1 Ct that was immobilized on an *N*-hydroxysuccinimide (NHS) column (GE Healthcare Bio-Sciences AB, Uppsala, Sweden).

Preparation of LDs. Lipid droplets (LDs) were prepared as described previously (26). Cells were pelleted by centrifugation at 1,500 rpm. The pellet was resuspended in hypotonic buffer (50 mM HEPES [pH 7.4], 1 mM EDTA, 2 mM $MgCl_2$) supplemented with a protease inhibitor cocktail (Nacalai Tesque, Kyoto, Japan) and was incubated for 10 min at 4°C. The suspension was homogenized with 30 strokes of a glass Dounce homogenizer using a tight-fitting pestle (Wheaton, Millville, NJ). A 1/10 volume of 10× isotonic buffer {0.2 M HEPES (pH 7.4), 1.2 M potassium acetate (KoAc), 40 mM magnesium acetate [$Mg(oAc)_2$], and 50 mM dithiothreitol (DTT)} was added to the homogenate. The nuclei were removed by centrifugation at 2,000 rpm for 10 min at 4°C. The supernatant was collected and centrifuged at 16,000 × *g* for 10 min at 4°C. The supernatant was mixed with an equal volume of 1.04 M sucrose in isotonic buffer (50 mM HEPES, 100 mM KCl, 2 mM $MgCl_2$, and protease inhibitor cocktail). The solution was set in a 13.2-ml Polyallomer centrifuge tube (Beckman Coulter, Brea, CA). One milliliter of isotonic buffer was loaded onto the sucrose mixture. The tube was centrifuged at 100,000 × *g* in an SW41Ti rotor (Beckman Coulter) for 1 h at 4°C. After the centrifugation, the LD fraction on the top of the gradient solution was recovered in phosphate-buffered saline (PBS). The collected LD fraction was used for Western blot analysis.

Western blot analysis. Cells were lysed in a buffer containing 50 mM Tris-HCl (pH 8.0), 150 mM NaCl, 4 mM EDTA, 1% Nonidet P-40, 0.1% sodium dodecyl sulfate (SDS), 1 mM DTT, and 1 mM phenylmethylsulfonyl fluoride. Supernatants from these lysates were subjected to SDS-polyacrylamide gel electrophoresis, followed by immunoblot analysis using anti-DDX3 (catalog no. 54257 [NT] and 5428 [IN]; Anaspec, San Jose, CA), anti-DDX6 (A300-460A; Bethyl Laboratories, Montgomery, TX), anti-adipose differentiation-related protein (ADFP; GTX110204; GeneTex, San Antonio, TX), anti-calnexin (NT; Stressgen, Ann Arbor, MI), anti-HCV core (CP-9 and CP-11; Institute of Immunology, Tokyo, Japan), anti-β-actin antibody (A5441; Sigma, St. Louis, MO), anti-ATX2/SCA2 antibody (A302-033A; Bethyl), anti-PABP (sc-32318 [10E10]; Santa Cruz Biotechnology, Santa Cruz, CA), anti-PABP (ab21060; Abcam, Cambridge, United Kingdom), anti-G3BP1 (611126; BD Transduction Laboratories, San Jose, CA), anti-LSM1 (LS-C97364, Life Span Biosciences, Seattle, WA), anti-HSP70 (610607; BD), anti-XRN1 (A300-443A; Bethyl), or anti-PATL1 antibody.

Immunofluorescence and confocal microscopic analysis. Cells were fixed in 3.6% formaldehyde in PBS, permeabilized in 0.1% NP-40 in PBS at room temperature, and incubated with anti-DDX3 antibody (54257 [NT] and 5428 [IN]; Anaspec), anti-DDX3X (LS-C64576; Life Span), anti-DDX6 (A300-460A; Bethyl), anti-HCV core (CP-9 and CP-11), anti-ATX2/SCA2 antibody (A302-033A; Bethyl), anti-ataxin-2 (611378; BD), anti-PABP (ab21060; Abcam), anti-G3BP1 (A302-033A; Bethyl), anti-LSM1 (LS-C97364; Life Span), anti-XRN1

(A300-443A; Bethyl), anti-Dcp2 (A302-597A; Bethyl), anti-human Ago2 (011-22033; Wako, Osaka, Japan), or anti-PATL1 antibody at a 1:300 dilution in PBS containing 3% bovine serum albumin (BSA) for 30 min at 37°C. The cells were then stained with fluorescein isothiocyanate (FITC)-conjugated anti-rabbit antibody (Jackson ImmunoResearch, West Grove, PA) at a 1:300 dilution in PBS containing BSA for 30 min at 37°C. Lipid droplets and nuclei were stained with borondipyrromethene (BODIPY) 493/503 (Molecular Probes, Invitrogen) and DAPI (4′,6-diamidino-2-phenylindole), respectively, for 15 min at room temperature. Following extensive washing in PBS, the cells were mounted onto slides using a mounting medium of 90% glycerin–10% PBS with 0.01% *p*-phenylenediamine added to reduce fading. Samples were viewed under a confocal laser scanning microscope (LSM510; Zeiss, Jena, Germany).

Statistical analysis. A statistical comparison of the infectivities of HCV in the culture supernatants between the knockdown cells and the control cells was performed by using the Student *t* test. *P* values of less than 0.05 were considered statistically significant. All error bars indicate standard deviations.

RESULTS

HCV infection hijacks the P-body components. To investigate the potential role of P-body components in the HCV life cycle, we first examined the alteration of the subcellular localization of DDX3 or DDX6 by HCV-JFH1 infection using confocal laser scanning microscopy as previously described (2), since both DDX3 and DDX6 were identified previously as P-body components (6). For this, we used HuH-7-derived RSc cells, in which cell culture-generated HCV-JFH1 (JFH1 strain of genotype 2a) (37) can infect and effectively replicate (3, 4, 23). HCV-JFH1-infected RSc cells at 60 h postinfection were stained with anti-HCV core antibody, anti-DDX3, and/or anti-DDX6. Lipid droplets (LDs) and nuclei were stained with BODIPY 493/503 and DAPI (4′,6-diamidino-2-phenylindole), respectively. Samples were viewed under a confocal laser scanning microscope. Although we observed that endogenous DDX3 localized in faint cytoplasmic foci in uninfected RSc cells, DDX3 relocalized, formed ringlike structures, and colocalized with the HCV core protein in response to HCV-JFH1 infection (Fig. 1A). On the other hand, endogenous DDX6 was localized in the evident cytoplasmic foci termed P bodies in the uninfected cells (Fig. 1A). DDX6 also relocalized, formed ringlike structures, and colocalized with the core protein in response to HCV-JFH1 infection (Fig. 1A). Although we failed to observe that most of the P bodies of DDX6 perfectly colocalized with DDX3 in uninfected RSc cells (Fig. 1B), we observed a few P bodies of DDX6 colocalized with DDX3 in the uninfected cells (Fig. 1B, arrowheads). Intriguingly, we found that endogenous DDX3 colocalized with endogenous DDX6 in HCV-JFH1-infected cells (Fig. 1B). To further confirm this finding, pHA-DDX3 (41) and pcDNA3-FLAG-DDX6 were cotransfected into 293FT cells. Consequently, we observed that hemagglutinin (HA)-DDX3 colocalized with FLAG-DDX6 in 293FT cells coexpressing HA-DDX3 and FLAG-DDX6 (Fig. 1B), suggesting cross talk of DDX3 with DDX6. Recently, LDs have been found to be involved in an important cytoplasmic organelle for HCV production (26). Indeed, both DDX3 and DDX6 were recruited around LDs in response to HCV infection, while these proteins did not colocalize with LDs in uninfected naïve RSc cells (Fig. 1C). Furthermore, both DDX3 and DDX6 accumulated in the LD fraction of the HCV-JFH1-infected RSc cells; however, we could not detect both proteins in the LD fraction from uninfected control cells (Fig. 1D), suggesting that DDX3 and DDX6 are recruited around LDs in response to HCV infection.

These results suggest that HCV-JFH1 infection disrupts P-body formation. Therefore, we further examined whether or not HCV-JFH1 disrupts the P-body formations of other microRNA effectors, including Ago2; the Sm-like protein Lsm1, which is a subunit of heptameric-ring Lsm1-7, involved in decapping; the 5′-to-3′ exonuclease Xrn1; the decapping activator PATL1; and the decapping enzyme DCP2 (6, 21, 30). As expected, HCV-JFH1 disrupted the P-body formations of Ago2, Lsm1, and Xrn1 as well as PATL1 (Fig. 2). Lsm1, Xrn1, or PATL1 relocalized, formed ringlike structures, and colocalized with the HCV core protein in response to HCV-JFH1 infection, whereas they were localized predominantly in P bodies in uninfected RSc cells (Fig. 2). In fact, we observed that DDX6 colocalized with Ago2, a P-body marker (Fig. 2). In contrast, HCV-JFH1 failed to disrupt the P-body formation of DCP2 (Fig. 2). Thus, these results suggest that HCV disrupts P-body formation through the hijacking of P-body components.

HCV hijacks stress granule components. Since Nonhoff et al. recently reported that DDX6 interacted with ataxin-2 (ATX2) (28), we examined the potential cross talk among DDX6, ATX2, and HCV. Although ATX2 and G3BP1, a well-known stress granule component (36), were dispersed in the cytoplasm at 37°C, both proteins formed discrete aggregates termed stress granules and colocalized with each other in response to heat shock at 43°C for 45 min, indicating that ATX2 is also stress granule component (Fig. 3A). We did not observe prominent colocalization between DDX6 and ATX2 at 37°C (Fig. 3B). In contrast, we found that DDX6 was recruited, juxtaposed, and partially colocalized with stress granules of ATX2 in response to heat shock at 43°C for 45 min in the uninfected RSc cells (Fig. 3B). Notably, ATX2 was recruited, formed the ring-like structures, and partially colocalized with DDX6 in response to HCV-JFH1 infection even at 37°C (Fig. 3B). Furthermore, we noticed that ATX2 was recruited around LDs in HCV-JFH1-infected cells at 72 h postinfection, while ATX2 did not colocalize with LDs in uninfected cells (Fig. 3C), suggesting the colocalization of ATX2 with the HCV core protein in infected cells. Indeed, ATX2 colocalized with the HCV core protein in HCV-JFH1-infected RSc cells at 37°C (Fig. 3D). Moreover, HCV-JFH1 infection induced the colocalization of the core protein with other stress granule components, G3BP1 or PABP1 as well as ATX2 (Fig. 4 and 5). To further confirm our findings, we examined the time course of the redistribution of DDX6 and G3BP1 after inoculation with HCV-JFH1. Consequently, we still detected the P-body formation of DDX6 and dispersed G3BP1 in the cytoplasm, and we did not observe a colocalization between the HCV core protein and DDX6 at 12 and 24 h postinfection (Fig. 4). In contrast, we found that the P-body formation of DDX6 began to be disrupted at 36 h postinfection (Fig. 4). Consistently, G3BP1 formed stress granules at 36 h postinfection (Fig. 4). We then noticed a ringlike formation of DDX6 or G3BP1 and colocalization with the HCV core protein after 48 h postinfection (Fig. 4), suggesting that the disruption of P-body formation and the hijacking of P-body and stress granule components occur in a late step of HCV infection.

We then examined whether or not HCV-JFH1 infection

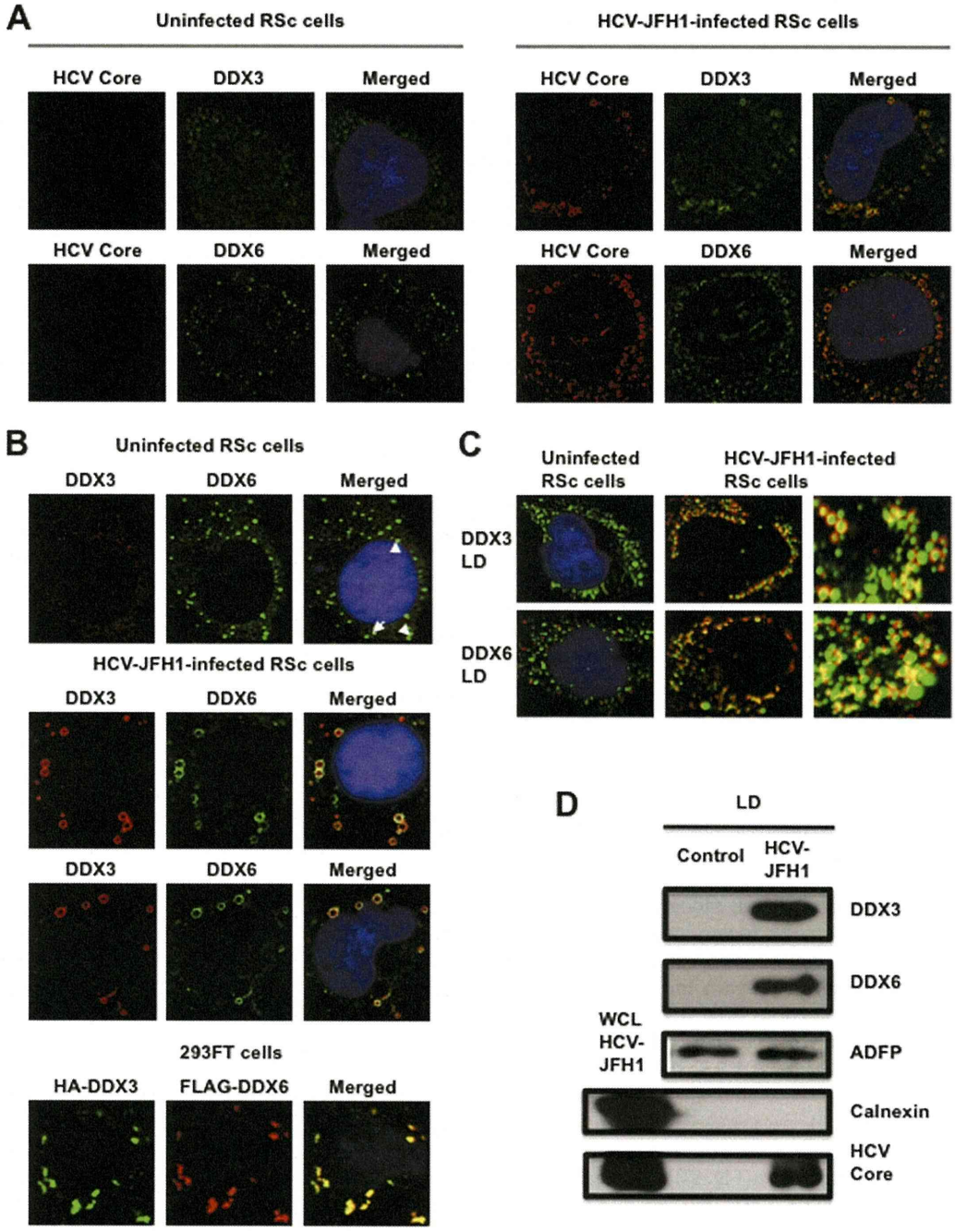

FIG. 1. Dynamic recruitment of DDX3 and DDX6 around lipid droplets (LDs) in response to HCV-JFH1 infection. (A) HCV-JFH1 disrupts the P-body formation of DDX6. Cells were fixed at 60 h postinfection and were then examined by confocal laser scanning microscopy. Cells were stained with anti-HCV core (CP-9 and CP-11 mixture) and either anti-DDX3 (54257 and 54258 mixture) or anti-DDX6 (A300-460A) antibody and then visualized with FITC (DDX3 or DDX6) or Cy3 (core). Images were visualized by using confocal laser scanning microscopy. The two-color overlay images are also exhibited (merged). Colocalization is shown in yellow. (B) HCV-JFH1 recruits DDX3 or DDX6 around LDs. Cells were stained with either anti-DDX3 or anti-DDX6 antibody and were then visualized with Cy3 (red). Lipid droplets and nuclei were stained with BODIPY 493/503 (green) and DAPI (blue), respectively. A high-magnification image is also shown. (C) Colocalization of DDX3 with DDX6. HCV-JFH1-infected RSc cells at 60 h postinfection were stained with anti-DDX3X (LS-C64576) and anti-DDX6 (A300-460A) antibodies. 293FT cells cotransfected with 100 ng of pcDNA3-FLAG-DDX6 and 100 ng of pHA-DDX3 (41) were stained with anti-FLAG-Cy3 and anti-HA-FITC antibodies (Sigma). (D) Association of DDX3 and DDX6 with LDs in response to HCV-JFH1 infection. The LD fraction and whole-cell lysates (WCL) were collected from uninfected RSc cells (control) or HCV-JFH1-infected RSc cells at 5 days postinfection. The results of Western blot analyses of DDX3, DDX6, and the HCV core protein as well as the LD marker ADFP and the endoplasmic reticulum (ER) marker calnexin in the LD fraction are shown.

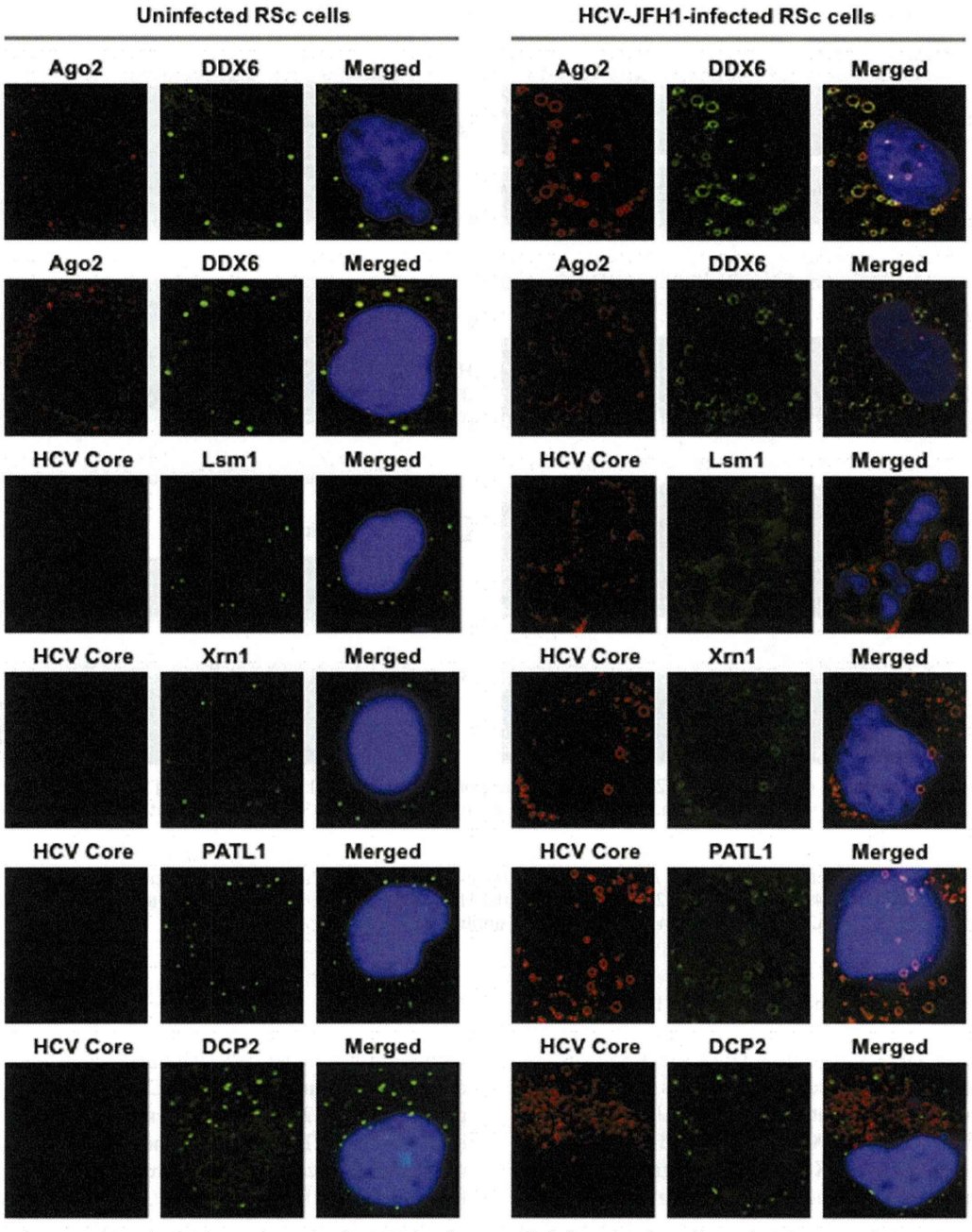

FIG. 2. HCV disrupts the P-body formation of microRNA effectors. Uninfected RSc cells and HCV-JFH1-infected RSc cells at 72 h postinfection were stained with anti-human AGO2 (011-22033) and anti-DDX6 (A300-460A) antibodies. The cells were also stained with anti-HCV core and anti-Lsm1 (LS-C97364), anti-Xrn1 (A300-443A), anti-PATL1, or anti-DCP2 (A302-597A) antibodies and were examined by confocal laser scanning microscopy.

could affect the stress granule formation of G3BP1, ATX2, or PABP1 in response to heat shock or treatment with arsenite. These stress granule components dispersed in the cytoplasm at 37°C, whereas these proteins formed stress granules in response to heat shock at 43°C for 45 min or treatment with 0.5 mM arsenite for 30 min (Fig. 5). In contrast, stress granules were not formed in HCV-JFH1-infected cells at 72 h postinfection in response to heat shock at 43°C for 45 min (Fig. 5), suggesting that HCV-JFH1 infection suppresses stress granule formation in response to heat shock or treatment with arsenite. Intriguingly, G3BP1, ATX2, or PABP1 still colocalized with the HCV core protein even under the above-described stress conditions (Fig. 5). Furthermore, Western blot analysis of cell lysates of uninfected or HCV-JFH1-infected cells at 72 h postinfection showed similar protein expression levels of ATX2, PABP1, HSP70, DDX3, DDX6, and Lsm1 but not G3BP1 (Fig. 6), suggesting that HCV-JFH1 infection does not affect host mRNA translation.

P-body and stress granule components are required for HCV replication. Finally, we investigated the potential role of

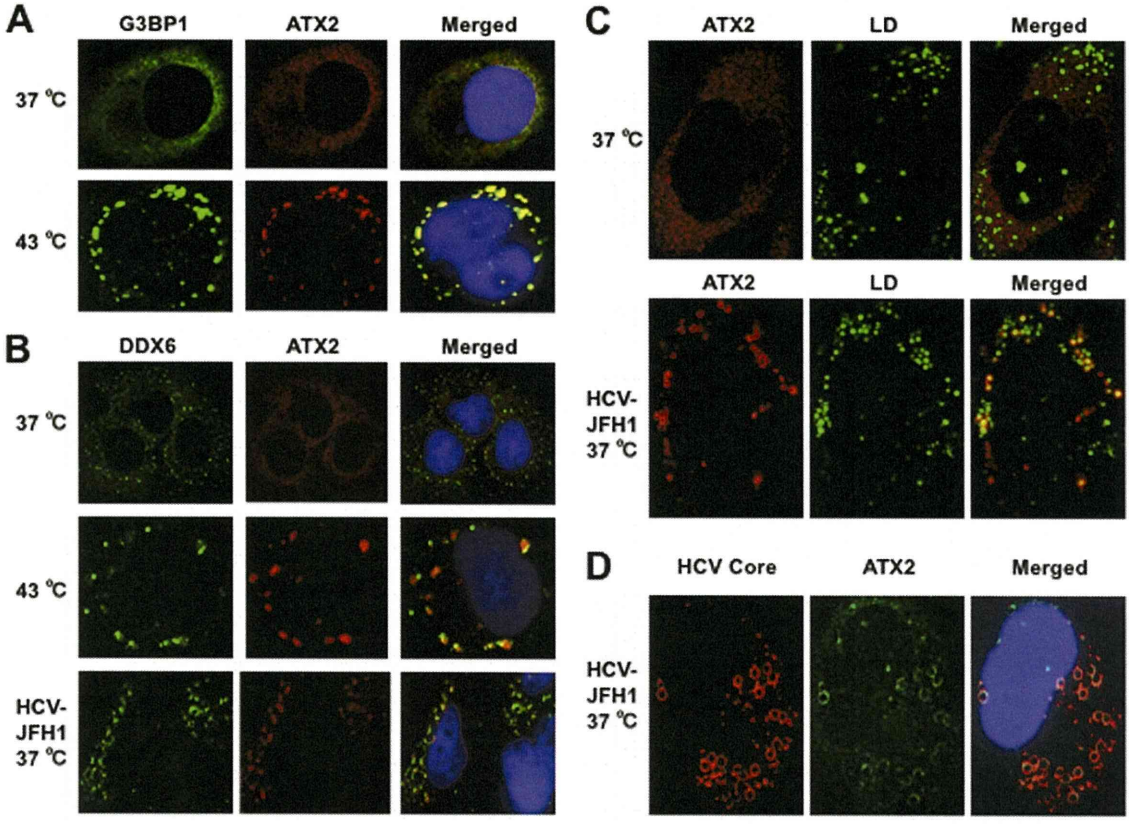

FIG. 3. Dynamic redistribution of ataxin-2 (ATX2) around LDs in response to HCV-JFH1 infection. (A) ATX2 is a stress granule component. RSc cells were incubated at 37°C or 43°C for 45 min. Cells were stained with anti-G3BP1 (A302-033A) and anti-ATX2 (A93520) antibodies and were examined by confocal laser scanning microscopy. (B) Dynamic redistribution of DDX6 and ATX2 in response to heat shock or HCV infection. RSc cells after heat shock at 43°C for 45 min or 72 h after inoculation with HCV-JFH1 were stained with anti-DDX6 and anti-ATX2 (A93520) antibodies. (C) HCV relocalizes ataxin-2 to LDs. HCV-JFH1-infected RSc cells at 72 h postinfection were stained with anti-ATX2 (A93520) antibody and BODIPY 493/503. (D) ATX2 colocalizes with the HCV core protein. HCV-JFH1-infected RSc cells at 72 h postinfection were stained with anti-ATX2/SCA2 (A301-118A) and anti-HCV core antibodies.

P-body and stress granule components in the HCV life cycle. We first used lentiviral vector-mediated RNA interference to stably knock down DDX6 as well as DDX3 in RSc cells. We used puromycin-resistant pooled cells 10 days after lentiviral transduction in all experiments. Real-time LightCycler RT-PCR analysis of DDX3 or DDX6 demonstrated a very effective knockdown of DDX3 or DDX6 in RSc cells transduced with lentiviral vectors expressing the corresponding shRNAs (Fig. 7A). Importantly, shRNAs did not affect cell viabilities (data not shown). We next examined the levels of HCV core and the infectivity of HCV in the culture supernatants as well as the level of intracellular HCV RNA in these knockdown cells 24 h after HCV-JFH1 infection at an MOI of 4. The results showed that the accumulation of HCV RNA was significantly suppressed in DDX3 or DDX6 knockdown cells (Fig. 7B). In this context, the release of the HCV core protein and the infectivity of HCV in the culture supernatants were also significantly suppressed in these knockdown cells (Fig. 7C and D). This finding suggested that DDX6 is required for HCV replication, like DDX3. To further examine the potential role of other P-body and stress granule components in HCV replication, we used RSc cells transiently transfected with a pool of siRNAs specific for ATX2, PABP1, Lsm1, Xrn1, G3BP1, and PATL1 as well as a pool of control siRNAs (siCon) following HCV-JFH1 infection. In spite of the very effective knockdown of each component (Fig. 7E), the siRNAs used in these experiments did not affect cell viabilities (data not shown). Consequently, the accumulation of HCV RNA was significantly suppressed in ATX2, PABP1, or Lsm1 knockdown cells (Fig. 7F), indicting that ATX2, PABP1, and Lsm1 are required for HCV replication. In contrast, the level of HCV RNA was not affected in Xrn1 knockdown cells (Fig. 7F), suggesting that Xrn1 is unrelated to HCV replication. Furthermore, we observed a moderate effect of siG3BP1 and siPATL1 on HCV RNA replication (Fig. 7F). Altogether, HCV seems to hijack the P-body and stress granule components around LDs for HCV replication.

DISCUSSION

So far, the P body and stress granules have been implicated in mRNA translation, RNA silencing, and RNA degradation as well as viral infection (1, 6, 22, 30). Host factors within the P body and stress granules can enhance or limit viral infection, and some viral RNAs and proteins accumulate in the P body and/or stress granules. Indeed, the microRNA effectors DDX6, GW182, Lsm1, and Xrn1 negatively regulate HIV-1 gene expression by preventing the association of viral mRNA

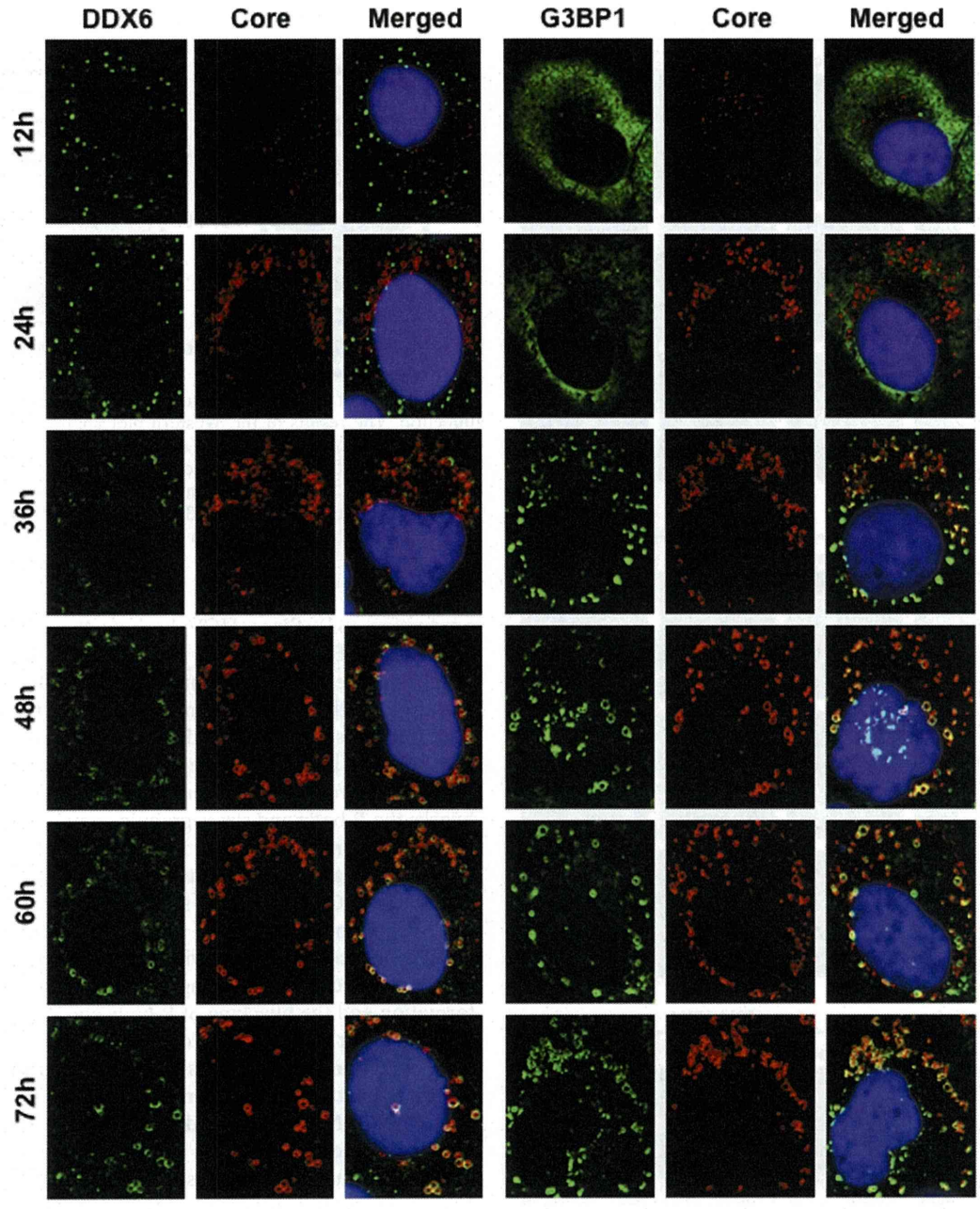

FIG. 4. Dynamic redistribution of DDX6 and G3BP1 in response to HCV-JFH1 infection. RSc cells at the indicated times (hours) after inoculation with HCV-JFH1 were stained with anti-HCV core and either anti-DDX6 (A300-460A) or anti-G3BP1 (A302-033A) antibodies.

with polysomes (9). In contrast, miRNA effectors such as DDX6, Lsm1, PatL1, and Ago2 positively regulate HCV replication (Fig. 7B and F) (16, 31, 33). We have also found that DDX3 and DDX6 are required for HCV RNA replication (3) (Fig. 7B) and that DDX3 colocalized with DDX6 in HCV-JFH1-infected RSc cells (Fig. 1B), suggesting that DDX3 comodulates the DDX6 function in HCV RNA replication. In this regard, the liver-specific miR-122 interacts with the 5′-UTR of the HCV RNA genome and positively regulates HCV replication (15, 17, 19, 20, 31). Since miRNAs usually interact with DDX6 and Ago2 in miRISC and are involved in RNA silencing, DDX6 and Ago2 may be required for miR-122-dependent HCV replication. Indeed, quite recently, a study showed that Ago2 is required for miR-122-dependent HCV RNA replication and translation (40). However, little is known regarding how miR-122 and DDX6 positively regulate HCV replication. Accordingly, we have shown that these miRNA effectors, including DDX6, Lsm1, Xrn1, and Ago2, accumulated around LDs and the HCV production factory and colocalized with the HCV core protein in response to HCV infection (Fig. 1 and 2). However, the decapping enzyme DCP2 did not accumulate and colocalize with the core protein (Fig. 2). Consistent with this finding, Scheller et al. reported previously that the depletion of DCP2 by siRNA did not affect HCV

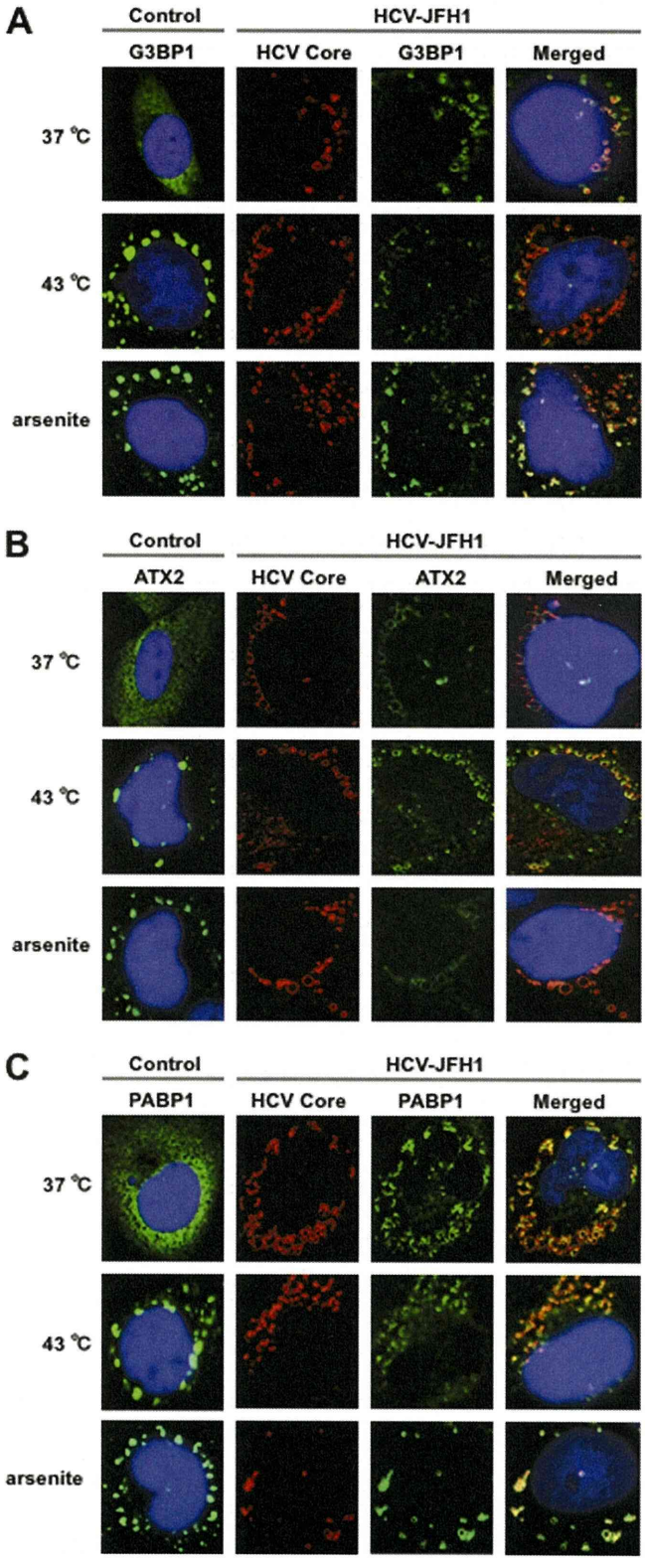

FIG. 5. HCV suppresses stress granule formation in response to heat shock or treatment with arsenite. Naïve RSc cells or HCV-JFH1-infected RSc cells at 72 h postinfection were incubated at 37°C or 43°C for 45 min. Cells were also treated with 0.5 mM arsenite for 30 min. Cells were stained with anti-HCV core and anti-G3BP1 (A), anti-ATX2 (B), or anti-PABP1 (ab21060) (C) antibodies and were examined by confocal laser scanning microscopy.

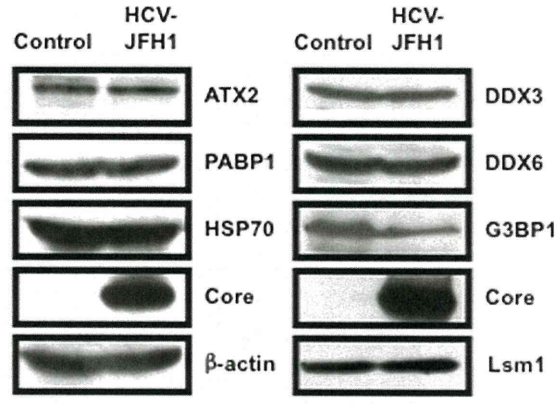

FIG. 6. Host protein expression levels in response to HCV-JFH1 infection. The results of the Western blot analyses of cellular lysates with anti-ATX2/SCA2 antibody (A301-118A), anti-PABP1 (ab21060), anti-HSP70 (610607), anti-HCV core, anti-β-actin, anti-DDX3 (54257 [NT] and 5428 [IN] mixture), anti-DDX6 (A300-460A), anti-G3BP1 (611126), or anti-LSM1 (LS-C97364) antibody in HCV-JFH1-infected RSc cells at 72 h postinfection as well as in naïve RSc cells are shown.

production (33). Since HCV harbors the internal ribosome entry site (IRES) structure in the 5′-UTR of the HCV genome instead of a cap structure, unlike HIV-1, DCP2 may not be recruited on the HCV genome and utilized for HCV replication. Otherwise, DCP2 may determine whether or not DDX6 and miRNAs positively or negatively regulate target mRNA.

Furthermore, we have demonstrated that HCV infection hijacks the P-body and stress granule components around LDs (Fig. 1, 2, 4, and 5). We have found that the P-body formation of DDX6 began to be disrupted at 36 h postinfection (Fig. 4). Consistently, G3BP1 formed stress granules at 36 h postinfection. We then observed the ringlike formation of DDX6 or G3BP1 and colocalization with the HCV core protein after 48 h postinfection, suggesting that the disruption of P-body formation and the hijacking of P-body and stress granule components occur at a late step of HCV infection. Furthermore, HCV infection could suppress stress granule formation in response to heat shock or treatment with arsenite (Fig. 5). In this regard, West Nile virus and dengue virus, of the family *Flaviviridae*, interfere with stress granule formation and P-body assembly through interactions with T cell intracellular antigen 1 (TIA-1)/TIAR (11). Moreover, PABP1 and G3BP1, stress granule components, are known to be common viral targets for the inhibition of host mRNA translation (34, 39). In fact, HIV-1 and poliovirus proteases cleave PABP1 and/or G3BP1 and suppress stress granule formation during viral infection (34, 39). On the other hand, HCV infection transiently induced stress granules at 36 h postinfection (Fig. 4) and did not cleave PABP1 (Fig. 6); however, HCV could suppress stress granule formation in response to heat shock or treatment with arsenite through hijacking their components around LDs, the HCV production factory (Fig. 5). Consistently, Jones et al. showed that HCV transiently induces stress granules of enhanced green fluorescent protein (EGFP)-G3BP at 36 h after infection with the cell culture-generated HCV (HCVcc) reporter virus Jc1FLAG2 (p7-nsGluc2A); however, those authors did not show the recruitment of EGFP-G3BP to LDs (18). Although we do not know the exact reason for this apparent discrepancy,

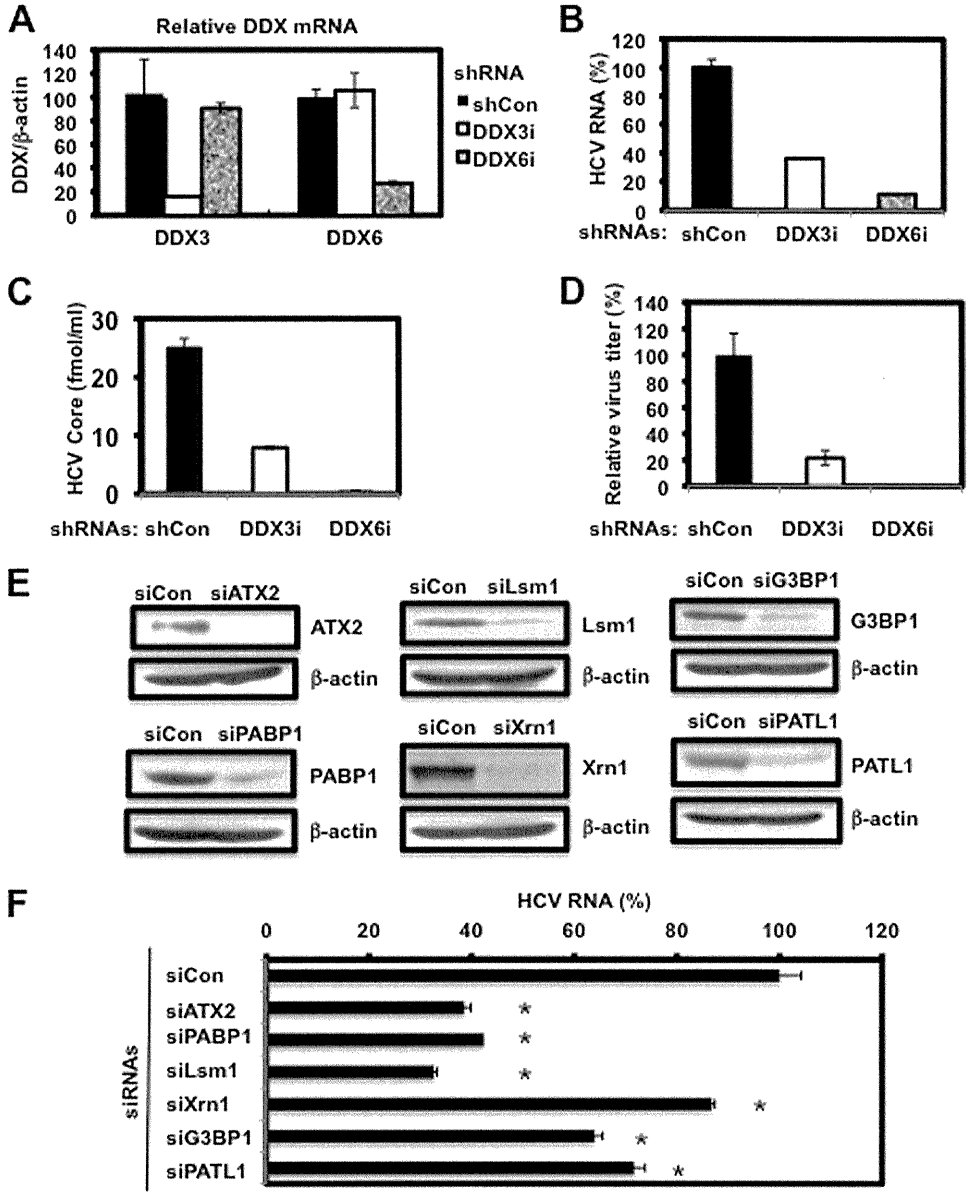

FIG. 7. Requirement of P-body and stress granule components for HCV replication. (A) Inhibition of DDX3 or DDX6 mRNA expression by the shRNA-producing lentiviral vector. Real-time LightCycler RT-PCR for DDX3 or DDX6 was also performed for β-actin mRNA in RSc cells expressing shRNA targeted to DDX3 (DDX3i) or DDX6 (DDX6i) or the control nontargeting shRNA (shCon) in triplicate. Each mRNA level was calculated relative to the level in RSc cells transduced with the control nontargeting lentiviral vector (shCon), which was assigned as 100%. Error bars in this panel and other panels indicate standard deviations. (B) Levels of intracellular genome-length HCV-JFH1 RNA in the cells at 24 h postinfection at an MOI of 4 were monitored by real-time LightCycler RT-PCR. Results from three independent experiments are shown. Each HCV RNA level was calculated relative to the level in RSc cells transduced with a control lentiviral vector (shCon), which was assigned as 100%. (C) The levels of HCV core in the culture supernatants from the stable knockdown RSc cells 24 h after inoculation of HCV-JFH1 at an MOI of 4 were determined by ELISA. Experiments were done in triplicate, and columns represent the mean core protein levels. (D) The infectivity of HCV in the culture supernatants from stable-knockdown RSc cells 24 h after inoculation of HCV-JFH1 at an MOI of 4 was determined by a focus-forming assay at 24 h postinfection. Experiments were done in triplicate, and each virus titer was calculated relative to the level in RSc cells transduced with a control lentiviral vector (shCon), which was assigned as 100%. (E) Inhibition of ATX2, PABP1, Lsm1, Xrn1, G3BP1, or PATL1 protein expression by 72 h after transient transfection of RSc cells with a pool of control nontargeting siRNA (siCon) or a pool of siRNAs specific for ATX2, PABP1, Lsm1, Xrn1, G3BP1, or PATL1 (25 nM), respectively. The results of Western blot analyses of cellular lysates with anti-ATX2, anti-PABP1, anti-Lsm1, anti-Xrn1, anti-G3BP1, anti-PATL1, or anti-β-actin antibody are shown. (F) Levels of intracellular genome-length HCV-JFH1 RNA in the cells at 48 h postinfection at an MOI of 1 were monitored by real-time LightCycler RT-PCR. RSc cells were transiently transfected with a pool of control siRNA (siCon) or a pool of siRNAs specific for ATX2, PABP1, Lsm1, Xrn1, G3BP1, and PATL1 (25 nM). At 48 h after transfection, the cells were inoculated with HCV-JFH1 at an MOI of 1 and incubated for 2 h. The culture medium was then changed and incubated for 22 h. Experiments were done in triplicate, and each HCV RNA level was calculated relative to the level in RSc cells transfected with a control siRNA (siCon), which was assigned as 100%. Asterisks indicate significant differences compared to the control treatment (*, $P < 0.01$).

several possible explanations can be offered. First, those authors examined the localization of EGFP-G3BP within 48 h postinfection, and we observed it at later times (Fig. 4). Second, they used only EGFP-tagged G3BP instead of endogenous G3BP1. Third, they used a Jc1FLAG2 (p7-nsGluc2A) clone, and an HCV-JFH1 clone could markedly induce the recruitment of the core protein to LDs compared to that of Jc1. Also, Jangra et al. failed to observe the recruitment of DDX6 to LDs at 2 days after infection with HJ3-5 virus (16). Accordingly, we also observed that most of the DDX6 still formed intact P bodies at earlier times (12 h or 24 h postinfection). Importantly, we observed the recruitment of DDX6 to LDs 48 h later (Fig. 4). Furthermore, those authors did not show the ringlike structure formation of the HJ3-5 core protein around LDs, unlike the JFH1 core protein that we used in this study. The interaction of the HCV core protein with DDX6 may explain the recruitment of P-body components to LDs. However, we do not yet know whether the P-body function(s) can be performed on LDs. At least, HCV infection did not affect the translation of several host mRNAs with 5′ caps and 3′ poly(A) tails despite the disruption of P-body formation at 72 h postinfection (Fig. 6), suggesting that HCV does not affect P-body function and that HCV recruits functional P bodies to LDs.

We need to address the potential role of stress granule components, such as PABP1, in HCV replication/translation, since the HCV genome does not harbor the 3′ poly(A) tail. Intriguingly, we have found that the accumulation of HCV RNA was significantly suppressed in PABP1 knockdown RSc cells (Fig. 7F). In this regard, Tingting et al. demonstrated previously that G3BP1 and PABP1 as well as DDX1 were identified as the HCV 3′-UTR RNA-binding proteins by proteomic analysis and that G3BP1 was required for HCV RNA replication (35). Yi et al. also reported that G3BP1 was associated with HCV NS5B and that G3BP1 was required for HCV RNA replication (42). We observed a moderate effect of siG3BP1 on HCV RNA replication (Fig. 7F). In contrast, the accumulation of HCV RNA was significantly suppressed in ATX2 and Lsm1 knockdown cells as well as in PABP1 knockdown cells (Fig. 7F), suggesting that ATX2, Lsm1, and PABP1 are required for HCV replication.

Taking these results together, this study has demonstrated for the first time that HCV hijacks P-body and stress granule components around LDs. This hijacking may regulate HCV RNA replication and translation. Indeed, we have found that the accumulation of genome-length HCV-O (genotype 1b) (14) RNA was markedly suppressed in DDX6 knockdown O cells (data not shown). More importantly, these P-body and stress granule components may be involved in the maintenance of the HCV RNA genome without 5′ cap and 3′ poly(A) tail structures in the cytoplasm for long periods, since the hijacking of P-body and stress granule components by HCV occurred at later times.

ACKNOWLEDGMENTS

We thank D. Trono for the lentiviral vector system, T. Wakita for HCV-JFH1, and K. T. Jeang for pHA-DDX3. We also thank T. Nakamura and K. Takeshita for their technical assistance.

This work was supported by a grant-in-aid for scientific research (C) from the Japan Society for the Promotion of Science (JSPS); by a grant-in-aid for research on hepatitis from the Ministry of Health, Labor, and Welfare of Japan; and by the Viral Hepatitis Research Foundation of Japan. M.K. was supported by a research fellowship from the JSPS for young scientists.

REFERENCES

1. **Anderson, P., and N. Kedersha.** 2007. Stress granules: the Tao of RNA triage. Trends Biochem. Sci. **33:**141–150.
2. **Ariumi, Y., et al.** 2003. Distinct nuclear body components, PML and SMRT, regulate the *trans*-acting function of HTLV-1 Tax oncoprotein. Oncogene **22:**1611–1619.
3. **Ariumi, Y., et al.** 2007. DDX3 DEAD-box RNA helicase is required for hepatitis C virus RNA replication. J. Virol. **81:**13922–13926.
4. **Ariumi, Y., et al.** 2008. The DNA damage sensors ataxia-telangiectasia mutated kinase and checkpoint kinase 2 are required for hepatitis C virus RNA replication. J. Virol. **82:**9639–9646.
5. **Ariumi, Y., et al.** 2011. The ESCRT system is required for hepatitis C virus production. PLoS One **6:**e14517.
6. **Beckham, C. J., and R. Parker.** 2008. P bodies, stress granules, and viral life cycles. Cell Host Microbe **3:**206–212.
7. **Bridge, A. J., S. Pebernard, A. Ducraux, A. L. Nicoulaz, and R. Iggo.** 2003. Induction of an interferon response by RNAi vectors in mammalian cells. Nat. Genet. **34:**263–264.
8. **Brummelkamp, T. R., R. Bernard, and R. Agami.** 2002. A system for stable expression of short interfering RNAs in mammalian cells. Science **296:**550–553.
9. **Chable-Bessia, C., et al.** 2009. Suppression of HIV-1 replication by microRNA effectors. Retrovirology **6:**26.
10. **Cristea, I. M., et al.** 2010. Host factors associated with the Sindbis virus RNA-dependent RNA polymerase: role for G3BP1 and G3BP2 in virus replication. J. Virol. **84:**6720–6732.
11. **Emara, M. M., and M. A. Brinton.** 2007. Interaction of TIA-1/TIAR with West Nile and dengue virus products in infected cells interferes with stress granule formation and processing body assembly. Proc. Natl. Acad. Sci. U. S. A. **104:**9041–9046.
12. **Hijikata, M., N. Kato, Y. Ootsuyama, M. Nakagawa, and K. Shimotohno.** 1991. Gene mapping of the putative structural region of the hepatitis C virus genome by in vitro processing analysis. Proc. Natl. Acad. Sci. U. S. A. **88:**5547–5551.
13. **Hijikata, M., et al.** 1993. Proteolytic processing and membrane association of putative nonstructural proteins of hepatitis C virus. Proc. Natl. Acad. Sci. U. S. A. **90:**10773–10777.
14. **Ikeda, M., et al.** 2005. Efficient replication of a full-length hepatitis C virus genome, strain O, in cell culture, and development of a luciferase reporter system. Biochem. Biophys. Res. Commun. **329:**1350–1359.
15. **Jangra, R. K., M. Yi, and S. M. Lemon.** 2010. Regulation of hepatitis C virus translation and infectious virus production by the microRNA miR-122. J. Virol. **84:**6615–6625.
16. **Jangra, R. K., M. Yi, and S. M. Lemon.** 2010. DDX6 (Rck/p54) is required for efficient hepatitis C virus replication but not IRES-directed translation. J. Virol. **84:**6810–6824.
17. **Ji, H., et al.** 2008. MicroRNA-122 stimulates translation of hepatitis C virus RNA. EMBO J. **27:**3300–3310.
18. **Jones, C. T., et al.** 2010. Real-time imaging of hepatitis C virus infection using a fluorescent cell-based reporter system. Nat. Biotechnol. **28:**167–171.
19. **Jopling, C. L., M. Yi, A. M. Lancaster, S. M. Lemon, and P. Sarnow.** 2005. Modulation of hepatitis C virus RNA abundance by a liver-specific microRNA. Science **309:**1577–1581.
20. **Jopling, C. L., S. Schütz, and P. Sarnow.** 2008. Position-dependent function for a tandem microRNA miR-122-binding site located in the hepatitis C virus RNA genome. Cell Host Microbe **4:**77–85.
21. **Kato, N., et al.** 1990. Molecular cloning of the human hepatitis C virus genome from Japanese patients with non-A, non-B hepatitis. Proc. Natl. Acad. Sci. U. S. A. **87:**9524–9528.
22. **Kedersha, N., and P. Anderson.** 2007. Mammalian stress granules and processing bodies. Methods Enzymol. **431:**61–81.
23. **Kuroki, M., et al.** 2009. Arsenic trioxide inhibits hepatitis C virus RNA replication through modulation of the glutathione redox system and oxidative stress. J. Virol. **83:**2338–2348.
24. **Kushima, Y., T. Wakita, and M. Hijikata.** 2010. A disulfide-bonded dimer of the core protein of hepatitis C virus is important for virus-like particle production. J. Virol. **84:**9118–9127.
25. **Mamiya, N., and H. J. Worman.** 1999. Hepatitis C virus core protein binds to a DEAD box RNA helicase. J. Biol. Chem. **274:**15751–15756.
26. **Miyanari, Y., et al.** 2007. The lipid droplet is an important organelle for hepatitis C virus production. Nat. Cell Biol. **9:**1089–1097.
27. **Naldini, L., et al.** 1996. In vivo gene delivery and stable transduction of nondividing cells by a lentiviral vector. Science **272:**263–267.
28. **Nonhoff, U., et al.** 2007. Ataxin-2 interacts with the DEAD/H-box RNA helicase DDX6 and interferes with P-bodies and stress granules. Mol. Biol. Cell **18:**1385–1396.
29. **Owsianka, A. M., and A. H. Patel.** 1999. Hepatitis C virus core protein interacts with a human DEAD box protein DDX3. Virology **257:**330–340.

30. **Parker, R., and U. Sheth.** 2007. P bodies and the control of mRNA translation and degradation. Mol. Cell **25:**635–646.
31. **Randall, G., et al.** 2007. Cellular cofactors affecting hepatitis C virus infection and replication. Proc. Natl. Acad. Sci. U. S. A. **104:**12884–12889.
32. **Rocak, S., and P. Linder.** 2004. DEAD-box proteins: the driving forces behind RNA metabolism. Nat. Rev. Mol. Cell Biol. **5:**232–241.
33. **Scheller, N., et al.** 2009. Translation and replication of hepatitis C virus genomic RNA depends on ancient cellular proteins that control mRNA fates. Proc. Natl. Acad. Sci. U. S. A. **106:**13517–13522.
34. **Smith, R. W., and N. K. Gray.** 2010. Poly(A)-binding protein (PABP): a common viral target. Biochem. J. **426:**1–11.
35. **Tingting, P., F. Caiyun, Y. Zhigang, Y. Pengyuan, and Y. Zhenghong.** 2006. Subproteomic analysis of the cellular proteins associated with the 3′ untranslated region of the hepatitis C virus genome in human liver cells. Biochem. Biophys. Res. Commun. **347:**683–691.
36. **Tourrière, H., et al.** 2003. The RasGAP-associated endoribonuclease G3BP assembles stress granules. J. Cell Biol. **160:**823–831.
37. **Wakita, T., et al.** 2005. Production of infectious hepatitis C virus in tissue culture from a cloned viral genome. Nat. Med. **11:**791–796.
38. **Weston, A., and J. Sommerville.** 2006. Xp54 and related (DDX6-like) RNA helicase: roles in messenger RNP assembly, translation regulation and RNA degradation. Nucleic Acids Res. **34:**3082–3094.
39. **White, J. P., A. M. Cardenas, W. E. Marissen, and R. E. Lloyd.** 2007. Inhibition of cytoplasmic mRNA stress granule formation by a viral proteinase. Cell Host Microbe **2:**295–305.
40. **Wilson, J. A., C. Zhang, A. Huys, and C. D. Richardson.** 2011. Human Ago2 is required for efficient miR-122 regulation of HCV RNA accumulation and translation. J. Virol. **85:**2342–2350.
41. **Yedavalli, V. S., C. Neuveut, Y. H. Chi, L. Kleiman, and K. T. Jeang.** 2004. Requirement of DDX3 DAED box RNA helicase for HIV-1 Rev-RRE export function. Cell **119:**381–392.
42. **Yi, Z., et al.** 2006. Subproteomic study of hepatitis C virus replicon reveals Ras-GTPase-activating protein binding protein 1 as potential HCV RC component. Biophys. Biochem. Res. Commun. **350:**174–178.
43. **You, L. R., et al.** 1999. Hepatitis C virus core protein interacts with cellular putative RNA helicase. J. Virol. **73:**2841–2853.
44. **Zufferey, R., D. Nagy, R. J. Mandel, L. Naldini, and D. Trono.** 1997. Multiply attenuated lentiviral vector achieves efficient gene delivery in vivo. Nat. Biotechnol. **15:**871–875.

Liver INTERNATIONAL
OFFICIAL JOURNAL OF THE INTERNATIONAL ASSOCIATION FOR THE STUDY OF THE LIVER

Liver International ISSN 1478-3223

BASIC STUDIES

Anti-ulcer agent teprenone inhibits hepatitis C virus replication: potential treatment for hepatitis C

Masanori Ikeda[1]*, Yoshinari Kawai[1,2]*, Kyoko Mori[1], Masahiko Yano[1,3], Ken-ichi Abe[1], Go Nishimura[1], Hiromichi Dansako[1], Yasuo Ariumi[1], Takaji Wakita[4], Kazuhide Yamamoto[2] and Nobuyuki Kato[1]

1 Department of Tumor Virology, Okayama University Graduate School of Medicine, Dentistry, and Pharmaceutical Sciences, Okayama, Japan
2 Department of Gastroenterology and Hepatology, Okayama University Graduate School of Medicine, Dentistry, and Pharmaceutical Sciences, Okayama, Japan
3 Division of Gastroenterology and Hepatology, Graduate School of Medical and Dental Sciences, Niigata University, Niigata City, Japan
4 Department of Virology II, National Institute of Infectious Diseases, Tokyo, Japan

Keywords
geranylgeranylation – HCV – Selbex – statin – teprenone

Correspondence
Masanori Ikeda, MD, PhD, Department of Tumor Virology, Okayama University Graduate School of Medicine, Dentistry, and Pharmaceutical Sciences, 2-5-1 Shikata-cho, Okayama 700-8558, Japan
Tel: +81-86-235-7386
Fax: +81-86-235-7392
e-mail: maikeda@md.okayama-u.ac.jp

Received 11 October 2010
Accepted 7 February 2011

DOI:10.1111/j.1478-3231.2011.02499.x

Abstract

Background: Previously we reported that 3-hydroxy-3-methylglutaryl coenzyme A reductase inhibitors, statins, inhibited hepatitis C virus (HCV) RNA replication. Furthermore, recent reports revealed that the statins are associated with a reduced risk of hepatocellular carcinoma and lower portal pressure in patients with cirrhosis. The statins exhibited anti-HCV activity by inhibiting geranylgeranylation of host proteins essential for HCV RNA replication. Geranylgeranyl pyrophosphate (GGPP) is a substrate for geranylgeranyltransferase. Therefore, we examined the potential of geranyl compounds with chemical structures similar to those of GGPP to inhibit HCV RNA replication. *Methods:* We tested geranyl compounds [geranylgeraniol, geranylgeranoic acid, vitamin K_2 and teprenone (Selbex)] for their effects on HCV RNA replication using genome-length HCV RNA-replicating cells (the OR6 assay system) and a JFH-1 infection cell culture system. Teprenone is the major component of the anti-ulcer agent, Selbex. We also examined the anti-HCV activities of the geranyl compounds in combination with interferon (IFN)-α or statins. *Results:* Among the geranyl compounds tested, only teprenone exhibited anti-HCV activity at a clinically achievable concentration. However, other anti-ulcer agents tested had no inhibitory effect on HCV RNA replication. The combination of teprenone and IFN-α exhibited a strong inhibitory effect on HCV RNA replication. Although teprenone alone did not inhibit geranylgeranylation, surprisingly, statins' inhibitory action against geranylgeranylation was enhanced by cotreatment with teprenone. *Conclusions:* The anti-ulcer agent teprenone inhibited HCV RNA replication and enhanced statins' inhibitory action against geranylgeranylation. This newly discovered function of teprenone may improve the treatment of HCV-associated liver diseases as an adjuvant to statins.

Hepatitis C virus (HCV) infection frequently causes persistent hepatitis and leads to cirrhosis and hepatocellular carcinoma (HCC). Currently, the combination therapy of pegylated interferon (IFN) with ribavirin is available for patients with chronic hepatitis C (CH C) and yields a sustained virological response rate of about 50% (1). However, about half of CH C patients are still susceptible to the progression of the disease to fatal cirrhosis and HCC. Therefore, the development of more effective reagents for the treatment of HCV infection is urgent.

To overcome this problem, we developed a genome-length HCV RNA (strain O of genotype 1b) replication system (OR6) with luciferase as a reporter, which facilitated the prompt and precise monitoring of HCV RNA replication in hepatoma cells (HuH-7-derived OR6 cells) (2). Using this OR6 system, we recently reported that 3-hydroxy-3-methylglutaryl coenzyme A (HMG-CoA) reductase inhibitors, statins, inhibited HCV RNA replication efficiently (3–5). Among five statins – fluvastatin (FLV), atorvastatin (ATV), simvastatin (SIV), pravastatin (PRV) and lovastatin (LOV) – FLV exhibited the strongest anti-HCV activity, while PRV had no effect on HCV RNA replication (3, 6). More recently, Bader *et al.* (7) demonstrated that FLV inhibited HCV RNA replication

*Contributed equally.